

Data fission: splitting a single data point

James Leiner¹ Boyan Duan² Larry Wasserman¹ Aaditya Ramdas¹
{jleiner,larry,aramdas}@stat.cmu.edu
boyand@google.com

¹Department of Statistics and Data Science, Carnegie Mellon University

²Google

December 1, 2022

Abstract

Suppose we observe a random vector X from some distribution in a known family with unknown parameters. We ask the following question: when is it possible to split X into two pieces $f(X)$ and $g(X)$ such that neither part is sufficient to reconstruct X by itself, but both together can recover X fully, and their joint distribution is tractable? One common solution to this problem when multiple samples of X are observed is data splitting, but [Rasines and Young \(2021\)](#) offers an alternative approach that uses additive Gaussian noise — this enables post-selection inference in finite samples for Gaussian distributed data and asymptotically for non-Gaussian additive models. In this paper, we offer a more general methodology for achieving such a split in finite samples by borrowing ideas from Bayesian inference to yield a (frequentist) solution that can be viewed as a continuous analog of data splitting. We call our method data fission, as an alternative to data splitting, data carving and p-value masking. We exemplify the method on several prototypical applications, such as post-selection inference for trend filtering and other regression problems, and effect size estimation after interactive multiple testing.

Contents

1	Introduction	2
1.1	An application: data fission for post-selection inference	3
1.2	Related work on data splitting and carving	5
2	Techniques to accomplish data fission	6
2.1	Achieving (P2) using “conjugate prior reversal”	6
2.2	Example decompositions	7
2.3	Relationship between data splitting and data fission	7
3	Application: selective CIs after interactive multiple testing	8
4	Application: selective CIs in fixed-design linear regression	10
5	Application to selective CIs in fixed-design generalized linear models and other quasi-MLE problems	13
5.1	Problem setup and a recap of QMLE methods	13
5.2	Simulation results	14
6	Application to post-selection inference for trend filtering and other nonparametric regression problems	15
6.1	Application to trend filtering	16
6.2	Application to spectroscopy	18

7 Conclusion	19
A Proofs and additional theoretical results	22
A.1 Proof of Theorem 1	22
A.2 Proof of Theorem 2	22
A.3 Proof of Corollary 1	22
A.4 Extension to unknown variance in Gaussian linear regression	22
A.5 Technical exposition of QMLE procedures	23
B List of decompositions	27
C Comparison between data splitting and data fission in fixed-design linear regression	30
D Background on trend filtering	30
E Supplemental simulation results	31
E.1 Simulation results for interactive hypothesis testing	31
E.2 Simulation results for fixed-design linear regression	34
E.3 Simulation results for fixed-design Poisson regression	36
E.4 Simulation results for fixed-design logistic regression	38
E.5 Simulation results for trend filtering	41
E.5.1 Additional results for pointwise CI simulations	42
E.5.2 Additional results for uniform CI simulations	42
E.5.3 Estimating variance before data fission	46
E.5.4 Alternative methods for selecting knots	47
F Additional empirical results for spectroscopy datasets	49

1 Introduction

One of the most common practices in applied statistics is data splitting. Given a dataset $X = (X_1, \dots, X_n)$ containing n independent samples, suppose an analyst wishes to divide the data into two smaller independent dataset in order to complete an analysis. The typical method for accomplishing this would be to choose m such that $1 \leq m < n$ and then form two new datasets: $f(X) = (X_1, \dots, X_m)$ and $g(X) = (X_{m+1}, \dots, X_n)$. However, there are alternative approaches for accomplishing this goal that may be preferable. As a simplified example, consider the setting where we only observe a single data point $X \sim N(0, 1)$, and we would like to “split” X into two parts such that each part contains some information about X , X can be reconstructed from both parts taken together, but neither part is sufficient by itself to reconstruct X , and yet the joint distribution of these two parts is known. The constraints mentioned in the previous sentence avoid trivial solutions like outputting $f(X) = X$ and $g(X) = 0$, or $f(X) = X/3$ and $g(X) = 2X/3$, and so on.

Luckily, this example has a simple solution with external randomization. Generate an independent $Z \sim N(0, 1)$, and set $f(X) = X + Z$ and $g(X) = X - Z$. One can then reconstruct X by addition (and Z by subtraction, but we care less about Z , which has no utility of its own). Just knowing one out of $f(X)$ or $g(X)$ does not allow one to reconstruct X , but both parts have nontrivial information about X because their mutual information with X is nonzero. We also know that $f(X)$ and $g(X)$ are actually independent, and their marginal distributions are also Gaussian, so their joint distribution is tractable and known. Previously, idea of adding and subtracting Gaussian noise has been employed for various goals in the literature, such as false discovery rate control in regression problems using the concept of Gaussian mirrors as discussed in [Xing et al. \(2021\)](#) and to estimate risk in the normal

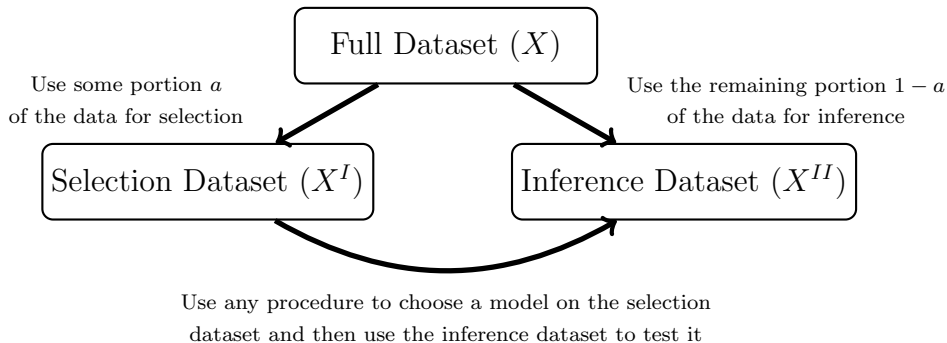


Figure 1. Illustration of typical **data splitting procedures** for post-selection inference. Splitting the data has the advantage of allowing the user to choose any selection strategy for model selection, but at the cost of decreased power during the inference stage.

means problem as discussed in [Oliveira et al. \(2021\)](#). Here we ask and answer different questions, with different goals in mind, and provide alternatives beyond the Gaussian case.

More generally, we seek to construct a family of pairs of functions $(f_\tau(X), g_\tau(X))_{\tau \in \mathcal{T}}$, for some totally ordered set \mathcal{T} (typically a subset of the real line), such that we can smoothly trade off the amount of information that each part contains about X . When τ approaches $\tau^+ := \sup\{\tau : \tau \in \mathcal{T}\}$, $f(X)$ will approach independence from X , while $g(X)$ will essentially equal X , but when τ approaches $\tau^- := \inf\{\tau : \tau \in \mathcal{T}\}$, the opposite will happen. To see how to do this, simply choose Z as before, and define $f(X) = X - \tau Z$ and $g(X) = X + \frac{Z}{\tau}$ and let $\mathcal{T} := (0, \infty)$. We call this procedure “data fission” because we divide X into two parts, each of which provides an independent yet complementary view of the original data.

Data fission is similar in spirit to data splitting. However, data fission manages to achieve the same effect from just a single sample X and not an n -dimensional vector. Nevertheless, the connection to data splitting is more than a mere analogy, and the exact relationship between τ and m can be quantified such that data fission is viewable as a continuous analog of data splitting in the Gaussian case; we do this in the next section.

Now, can the above ideas be generalized to other distributions? In other words, can we employ external randomization to “split” a single data point into two nontrivial parts when the distribution P is not Gaussian? This is the topic of study for the rest of this paper. We provide a positive answer when P is conjugate (in the standard Bayesian sense) to some other distribution Q , where the latter will be used (along with X) to determine the external randomization. In most cases, $f(X)$ and $g(X)$ will not simply be the sum/difference of X with some Z ; such a form was achieved only in the Gaussian case. Similarly, $f(X)$ and $g(X)$ will typically not be independent. Nevertheless, they will satisfy the conditions set out in the first paragraph of the paper and can be treated for inferential purposes as single sample variants of data splitting, justifying the title of the paper.

1.1 An application: data fission for post-selection inference

We primarily focus on demonstrating the applicability of these ideas in the context of (potentially high-dimensional) model selection and post-selection inference. With data splitting, the analyst picks some fraction $a \in \{\frac{1}{n}, \dots, \frac{n-1}{n}, 1\}$ of the data to use for model selection and the remaining $1 - a$ fraction to use for inference as illustrated in [Figure 1](#). Data fission is similar in spirit to this idea but instead uses randomization so that part of the information contained in every data point is used for both selection and inference. The procedure broadly works in three stages.

1. Split X into $f(X)$ and $g(X)$ such that $g(X)|f(X)$ is tractable to compute. The parameter τ controls the proportion of the information to be used for model selection.

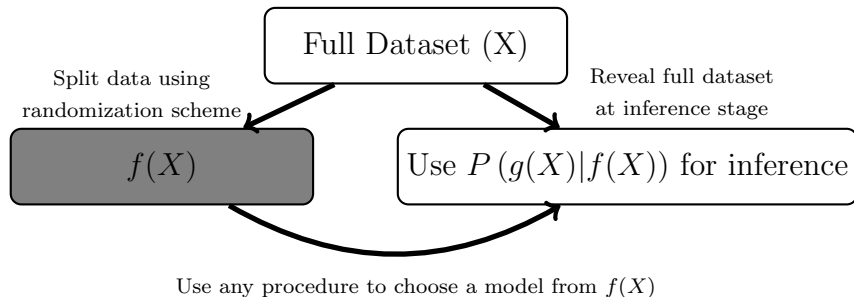


Figure 2. Illustration of the proposed **data fission** procedure. Similar to data splitting, it allows for any selection procedure for choosing the model. However, it achieves this through randomization rather than a direct splitting of the data.

2. Use $f(X)$ to select a model and/or hypotheses to test using any procedure available.
3. Use $g(X)|f(X)$ to test hypotheses and/or perform inference.

See Figure 2 for a graphical representation of the above steps. This approach can be viewed as a generalization of the methodologies discussed in Tian and Taylor (2018) and Rasines and Young (2021). In the above framework, these approaches amounts to letting $f(X) = X + \gamma Z$ and $g(X) = X$ with $Z \sim N(0, \sigma^2)$ for some fixed constant $\gamma > 0$. In the case where $X \sim N(\mu, \sigma^2)$ with known σ^2 , the authors show that $g(X)|f(X)$ has a tractable finite sample distribution. In cases where X is non-Gaussian, however, $g(X)|f(X)$ is only described asymptotically. In the next section, we will explore alternative ways to construct $g(X)$ that result in tractable finite sample distributions for non-Gaussian data.

In some ways, these methodologies can be seen as a compromise between data splitting and the approach of *data carving* as introduced in Fithian et al. (2014). Data carving, as illustrated in Figure 3, improves on data splitting in cases where the conditional distribution of the data given a selection event is known by including the leftover portion of Fisher information that was not used to inform the model choice in the inference procedure. A key limitation of this approach, however, is that it confines the analyst to model selection techniques with tractable post-selective distributions, such as the LASSO as described by Lee et al. (2016) or more general sequential regression procedures such as those discussed in Tibshirani et al. (2016). In many settings, ad-hoc exploratory data analyses such as the plotting of data or removal of outliers are ubiquitous and make data carving intractable.

Although data fission conditions on $f(X)$ rather than the selection event itself, it retains some similarities to data carving insofar as it uses a portion of every data point to inform both selection and inference. This has advantages relative to data splitting in at least two distinct ways. First, certain settings that involve sparse or rarely occurring features may result in a handful of data points having a disproportionate amount of influence — data fission allows for the analyst to “hedge their bets” by including these points in both the selection and inference steps. Second, in settings where the selected model is defined relative to a set of *fixed* covariates, the theoretical justification for data splitting becomes less clear conceptually. (In a fixed- X setup, how can a model that has been selected based on its ability to estimate the conditional distribution $Y | X^{\text{firsthalf}}$ also be understood to model the distribution that conditions on the other half of the split dataset $Y | X^{\text{secondhalf}}$?) For example, consider a time series dataset, where splitting a sample may require the analyst to have a selection and inference dataset that span entirely different time periods, or graph data where there is only one observation available for each location on a graph. On the other hand, similar to data splitting, data fission affords the analyst complete flexibility in how they choose their model based on the information revealed in the selection stage. In particular, the procedure can accommodate a model selection process that relies on qualitative or heuristic methods such as visual examination of residual plots or the consultation of domain experts to determine plausibility of the discovered relationships.

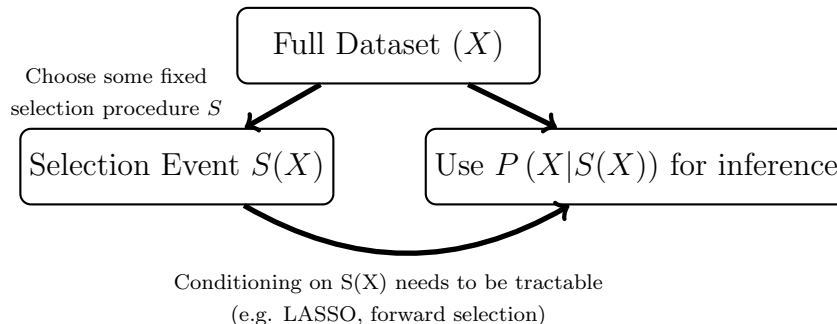


Figure 3. Illustration of **data carving procedure** as discussed in [Fithian et al. \(2014\)](#). Data carving has the advantage of using all unused information for inference, but requires the selection procedure to be *fixed* at the onset of investigation. Moreover, computing the conditional distribution needs to be tractable, either in closed form (e.g. LASSO as described in [Lee et al. \(2016\)](#)) or through numerical simulation. Thus data carving and fission have complementary benefits and tradeoffs.

Although we anticipate that these ideas may have other downstream applications beyond selective inference such as data privacy (including differential privacy), creation of fake (synthetic) datasets, and comparing machine learning algorithms, these require new techniques that are out of the scope of the current work.

1.2 Related work on data splitting and carving

Our work is influenced by the existing literature on procedures for selective inference after model selection. Although data splitting is perhaps the oldest and most commonly used method for ensuring valid coverage guarantees after model selection, rigorous examination of data splitting has only recently emerged in the literature. [Rinaldo et al. \(2019\)](#) is one such example where the authors examine data splitting in an assumption-lean context.

The idea of adding randomization for selective inference is discussed in [Tian and Taylor \(2018\)](#) for Gaussian data. They introduce a noise variable that is independent of the original data, and involve it at various stages of the selection procedure (e.g., introducing perturbations to the gradient when using LASSO to select features). Instead, we choose to construct a new random variable $f(X)$ that depends on X but is not exactly equal to X , and perform arbitrary selection procedures on $f(X)$.

Randomization was also used in [Li and Fithian \(2021\)](#) to recast the knockoff procedure of [Barber and Candès \(2015\)](#) as a selective inference procedure for the linear Gaussian model that adds noise to the OLS estimates $(\hat{\beta})$ to create a “whitened” version of $\hat{\beta}$ to use for hypothesis selection. The work of [Sarkar and Tang \(2021\)](#) explores similar ways of using knockoffs to split $\hat{\beta}$ into independent pieces for hypothesis selection but uses a deterministic splitting procedure. Although conceptually quite similar to our approach, these methods focus on splitting the coefficient estimates for a *fixed model* into two independent pieces and then adaptively choosing the hypotheses to test during the inference stage. As such, it is most naturally applied in low dimensional settings where model selection is less necessary. Similar randomization schemes for Gaussian distributed data are also explored in [Ignatiadis et al. \(2021\)](#) but are used for empirical Bayes procedures and not selective inference.

Outline of the paper. The general methodology for data fission is introduced in [Section 2](#). We illustrate how the procedure is used in the context of Gaussian data but then generalize this for the broader class of distributions where the data has a known conjugate prior. Examples are given across a variety of distributions commonly used for regression and data analysis such as Gaussian, Poisson, and Binomial. The remainder of the paper explores the use of data fission for four different applications: selective CIs after interactive multiple testing in [Section 3](#), fixed-design linear regression in [Section 4](#),

fixed-design generalized linear models in [Section 5](#), and trend filtering in [Section 6](#). Proofs for all theoretical results are omitted from the main body but included in [Appendix A](#).

A key limitation within all of these applications — shared by much of classical statistics and conditional inference — is that theoretical guarantees can only be given under correct specification of the distribution of errors due to the need to ensure that the post-selective distribution is known and tractable. However, these guarantees are still assumption-lean in the sense of assuming an unknown form for the conditional mean μ . Situations where the variance is unknown and is estimated before data fission in the Gaussian case are discussed in low dimensional settings, but we leave theoretical guarantees in higher dimensions as an open avenue for future investigation. We provide some concluding remarks in [Section 7](#).

2 Techniques to accomplish data fission

With statistical inference in mind, we explore decompositions of X to $f(X)$ and $g(X)$ such that both parts contain information about a parameter θ of interest, and there exists some function h such that $X = h(f(X), g(X))$, and with either of the following two properties:

- (P1). $f(X)$ and $g(X)$ are independent with known distributions (up to the unknown θ); or
- (P2). $f(X)$ has a known marginal distribution and $g(X)$ has a known conditional distribution given $f(X)$ (up to knowledge of θ).

The former property implies the latter and the former is generally more tractable. We explore alternative formulations that require weaker assumptions in [Section 5](#).

2.1 Achieving (P2) using “conjugate prior reversal”

Suppose X follows a distribution that is a conjugate prior distribution of the parameter in some likelihood. We then construct a new random variable Z following that likelihood (with the parameter being X). Letting $f(X) = Z$ and $g(X) = X$, the conditional distribution of $g(X) | f(X)$ will have the same form as X (with a different parameter depending on the value of $f(X)$). For example, suppose $X \sim \text{Exp}(\theta)$, which is conjugate prior to the Poisson distribution. Thus, we draw $Z = (Z_1, \dots, Z_B)$ where each element is i.i.d. $Z_i \sim \text{Poi}(X)$ and $B \in \{1, 2, \dots\}$ is a tuning parameter. Let $f(X) = Z$ and $g(X) = X$. Then, the conditional distribution of $g(X) | f(X)$ is $\text{Gamma}(1 + \sum_{i=1}^B f_i(X), \theta + B)$. On the other hand, $f(X) \sim \text{Geo}(\frac{\theta}{\theta+B})$. Larger B results in a more informative $f(X)$. More examples of such decompositions, which we term “conjugate prior reversal”, are in [Appendix B](#).

For exponential family distributions, we can construct $f(X)$ and $g(X)$ as follows.

Theorem 1. *Suppose that for some $A(\cdot, \cdot), \theta_1, \theta_2, H(\cdot, \cdot)$, the density of X is given by*

$$p(x | \theta_1, \theta_2) = H(\theta_1, \theta_2) \exp\{\theta_1^T x - \theta_2^T A(x)\}. \quad (1)$$

Suppose also that we can find $h(\cdot), T(\cdot)$ and θ_3 such that

$$p(z | x, \theta_3) = h(z) \exp\{x^T T(z) - \theta_3^T A(x)\} \quad (2)$$

is a well-defined distribution. First, draw $Z \sim p(z|X)$, and let $f(X) := Z$ and $g(X) := X$. Then, $(f(X), g(X))$ satisfy the data fission property (P2). Specifically, note that $f(X)$ has a known marginal distribution $p(z|\theta_1, \theta_2, \theta_3) = h(z) \frac{H(\theta_1, \theta_2)}{H(\theta_1 + T(z), \theta_2 + \theta_3)}$, while $g(X)$ has a known conditional distribution given $f(X)$, which is $p(x | z, \theta_1, \theta_2, \theta_3) = p(x | \theta_1 + T(z), \theta_2 + \theta_3)$.

Recall that all proofs are in [Appendix A](#).

Remark 1 (Trading off information in f and g). As an extension to the above result, we can draw B samples independently from (2) denoted as Z_i for $i \in [B]$, in which case $f(X) = Z \equiv \{Z_1, \dots, Z_B\}$ has marginal distribution

$$p(z|\theta_1, \theta_2, \theta_3) = \left[\prod_{i=1}^B h(z_i) \right] \frac{H(\theta_1, \theta_2)}{H(\theta_1 + \sum_{i=1}^B T(z_i), \theta_2 + B\theta_3)},$$

and $g(X) = X$ has conditional distribution as

$$p(x | z, \theta_1, \theta_2, \theta_3) = p(x | \theta_1 + \sum_{i=1}^B T(z_i), \theta_2 + B\theta_3).$$

Larger B indicates more information in $f(X)$, and thus less left over in $g(X)$.

2.2 Example decompositions

Below, we draw attention to techniques used in Sections 3, 4, 5, and 6.

- **Gaussian.** Suppose $X \sim N(\mu, \Sigma)$ is d -dimensional ($d \geq 1$). Draw $Z \sim N(0, \Sigma)$. Then $f(X) = X + \tau Z$, where $\tau \in (0, \infty)$ is a tuning parameter, has distribution $N(\mu, (1 + \tau^2)\Sigma)$; and $g(X) = X - \frac{1}{\tau}Z$ has distribution $N(\mu, (1 + \tau^{-2})\Sigma)$; and $f(X) \perp g(X)$. Larger τ indicates less informative $f(X)$ (and more informative $g(X) | f(X)$).
- **Bernoulli (P2).** Suppose $X \sim \text{Ber}(\theta)$. Draw $Z \sim \text{Ber}(p)$ where $p \in (0, 1)$ is a tuning parameter. Then $f(X) = X(1 - Z) + (1 - X)Z$ has marginal distribution $\text{Ber}(\theta + p - 2p\theta)$; and $g(X) = X$ has conditional distribution (given $f(X)$) as $\text{Ber}\left(\frac{\theta}{\theta + (1-\theta)[p/(1-p)]^{2f(X)-1}}\right)$. Smaller p indicates more information in $f(X)$.
- **Poisson.** Suppose $X \sim \text{Poi}(\mu)$. Fix parameter $p \in (0, 1)$ and draw $Z \sim \text{Bin}(X, p)$. Then $f(X) = Z$ has marginal distribution $\text{Poi}(p\mu)$; and $g(X) = X - Z$ is independent of $f(X)$ and has distribution $\text{Poi}((1 - p)\mu)$. Larger p indicates more informative $f(X)$.

A larger (but still incomplete) list of decomposition strategies for specific distributions is available in Appendix B. We encourage the reader to consult this list in order to get a full appreciation for the applicability of this approach to disparate problems in statistics.

2.3 Relationship between data splitting and data fission

A natural question is under which conditions data fission yields equivalent estimators as data splitting. One way to answer this is to examine when the proportion of Fisher information that is allocated to inference is the same for each approach.

Suppose we are given n i.i.d. observations $X = (X_1, \dots, X_n)$, where $X_i \sim p(\theta)$. The data splitting approach chooses S as a random subset of $[n]$ of size a where $a \in \{\frac{1}{n}, \dots, \frac{n-1}{n}, 1\}$ is a tuning parameter. Letting $\mathcal{I}_X(\theta)$ denote the Fisher information for the complete sample and $\mathcal{I}_1(\theta)$ denote the Fisher information for a single observation, we then have

$$\mathcal{I}_X(\theta) = \underbrace{an\mathcal{I}_1(\theta)}_{\text{Used for selection}} + \underbrace{(1 - an)\mathcal{I}_1(\theta)}_{\text{Used for inference}}.$$

For data fission, note the following identity for smooth parametric models: $\nabla^2 \ell(\theta|X) = \nabla^2 \ell(\theta; f(X)) + \nabla^2 \ell(\theta; g(X) | f(X))$. Taking expectations, and denoting $\mathcal{I}_{f(X)}$, $\mathcal{I}_{g(X)|f(X)}$ as the Fisher information

for the selection and inference datasets yields

$$\begin{aligned} \mathcal{I}_X(\theta) &= \mathcal{I}_{f(X)}(\theta) + \mathbb{E}[-\nabla^2 \ell(\theta; g(X) | f(X))] \\ &= \mathcal{I}_{f(X)}(\theta) + \mathbb{E}[-\mathbb{E}[\nabla^2 \ell(\theta; g(X) | f(X)) | f(X)]] = \underbrace{\mathcal{I}_{f(X)}(\theta)}_{\text{for selection}} + \underbrace{\mathbb{E}[\mathcal{I}_{g(X)|f(X)}(\theta)]}_{\text{for inference}}. \end{aligned}$$

For a fixed parameter a in data splitting, one can choose τ such that $\mathbb{E}[\mathcal{I}_{g(X)|f(X)}(\theta)] = (1 - an)\mathcal{I}_1(\theta)$ to find a comparable information split for data fission. This selected τ will only guarantee that the inference datasets created by data splitting and data fission approach contain the same information in expectation. For any particular realization of the fission step, $\mathcal{I}_{g(X)|f(X)}$ may be different than $(1 - an)\mathcal{I}_1(\theta)$. In situations where $g(X)$ and $f(X)$ are independent, this equality can be modified to hold exactly since $\mathbb{E}[\mathcal{I}_{g(X)|f(X)}(\theta)] = \mathcal{I}_{g(X)}$.

An important caveat is that this comparison only applies when the Fisher information is not a function of unknown parameters. Luckily, for Gaussians with known variance, this caveat does not apply. This justifies the informal assertion in [Section 1](#) that data fission for Gaussians can be viewed as a continuous analog of data splitting.

Example 1 (Gaussian Datasets). *Let $\{X_i\}_{i < n}$ be iid $N(\theta, \sigma^2)$. Recall that data splitting defines $f(X)$ and $g(X)$ as $f^{\text{split}}(X) = \frac{1}{an} \sum_{i \in S} X_i$ and $g^{\text{split}}(X) = \frac{1}{(1-a)n} \sum_{i \notin S} X_i$. Then:*

$$f^{\text{split}}(X) \sim N\left(\theta, \frac{1}{an}\right), \quad g^{\text{split}}(X) \sim N\left(\theta, \frac{1}{(1-a)n}\right), \quad f^{\text{split}}(X) \perp\!\!\!\perp g^{\text{split}}(X).$$

Larger a leads to more information in $f(X)$ and less in $g(X)$. Alternatively, the data fission approach decomposes each observation X_i as $f(X_i)$ and $g(X_i)$. We first simulate $\{Z_i\}_{i=1}^n$ distributed as i.i.d. $N(0, \sigma^2)$, and define $f(X_i)$ and $g(X_i)$ as $f^{\text{fission}}(X_i) := X_i + \tau Z_i$ and $g^{\text{fission}}(X_i) := X_i - \frac{1}{\tau} Z_i$ where $\tau \in (0, \infty)$ is a tuning parameter. This yields:

$$f^{\text{fission}}(X_i) \sim N\left(\theta, \sigma^2(1 + \tau^2)\right), \quad g^{\text{fission}}(X_i) \sim N\left(\theta, \sigma^2\left(1 + \frac{1}{\tau^2}\right)\right), \quad f^{\text{fission}}(X_i) \perp\!\!\!\perp g^{\text{fission}}(X_i).$$

Averaging all of these data points together gives us that $f^{\text{fission}}(X) = \frac{1}{n} \sum_{i=1}^n f^{\text{fission}}(X_i)$ and $g^{\text{fission}}(X) = \frac{1}{n} \sum_{i=1}^n g^{\text{fission}}(X_i)$. Equating the Fisher information of $f^{\text{fission}}(X)$ and $f^{\text{split}}(X)$ is equivalent to equating the variances. Therefore, to compare the two approaches, we can find the values of a, τ that result in $f(X)$ and $g(X)$ having the same variance. This results in the relation $a = \frac{1}{1 + \tau^2}$. For example, $a = 0.5$ corresponds to $\tau = 1$.

The above discussion assumes the parameter of interest θ is fixed prior to fissioning the data. When the selection dataset is used to decide which parameter to conduct inference on, this calculation is to be regarded as a heuristic.

Remark 2 (Trading information between f and g , part II). *In the list of decompositions and in [Remark 1](#) we noted that we could trade off “information” between $f(X)$ and $g(X)$ by varying certain hyperparameters. We can now clarify what this means. For a hyperparameter $p \in (a, b)$, we say that larger p corresponds to more informative $f(X)$ and less informative $g(X)|f(X)$ to mean that $\lim_{p \rightarrow b} \mathcal{I}_{f(X)}(\theta) = \mathcal{I}_X(\theta)$ and $\lim_{p \rightarrow b} \mathbb{E}[\mathcal{I}_{g(X)|f(X)}(\theta)] = 0$.*

3 Application: selective CIs after interactive multiple testing

Suppose we observe $y_i \sim N(\mu_i, \sigma^2), i \in [1, n]$ with known σ^2 alongside generic covariates $x_i \in \mathcal{X}$. After observing the data, the analyst has two goals. First, the analyst wishes to choose a subset of hypotheses \mathcal{R} to reject from the set $\{H_{0,i} : \theta_i = 0\}$ while controlling the false discovery rate (FDR),

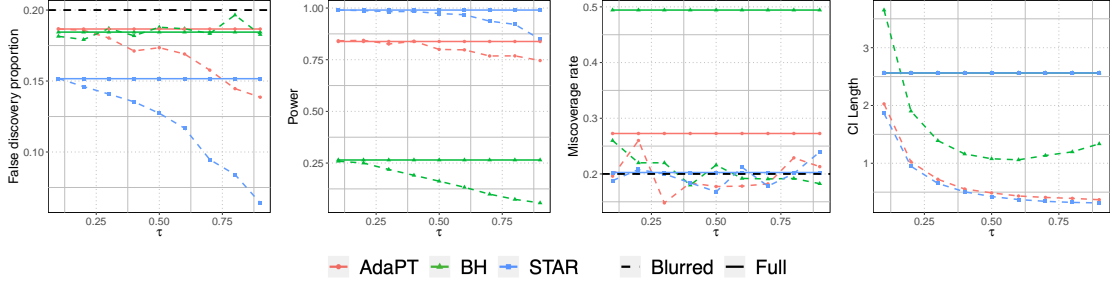


Figure 4. Numerical results averaged over 250 trials for a 50×50 grid of hypotheses with target FDR level chosen at 0.2 and τ varying over $\{0.1, 0.2, 0.3, 0.5, 0.5, 0.6, 0.7, 0.8, 0.9\}$. Solid lines denote metrics for the rejection sets formed using the full dataset and dotted lines denote metrics calculated using the rejection sets formed through data fission. All methods control the false discovery rate at the desired coverage level, but “double dipping” to form CIs after forming a rejection set using the full data results in invalid coverage. Fissioned CIs have the desired coverage and we see that the CI length generally decreases as τ increases because more of the dataset gets reserved for inference.

which is defined as the expected value of the false discovery proportion (FDP) $:= \frac{|\{x_i \in \mathcal{R}: \mu_i = 0\}|}{\max\{|\mathcal{R}|, 1\}}$. After selecting these hypotheses, the analyst then may wish to construct either:

- multiple confidence intervals (CIs) with $1 - \alpha$ coverage of μ_i for each $i \in \mathcal{R}$; or
- a single CI with $1 - \alpha$ coverage of $\bar{\mu} = \frac{1}{|\mathcal{R}|} \sum_{i \in \mathcal{R}} \mu_i$.

One method for rejecting hypotheses and constructing selective CIs that achieves coverage for the individual μ_i would be the BH procedure of [Benjamini and Hochberg \(1995\)](#) to form the rejection set and then construct CIs with $1 - \alpha$ coverage as described by [Benjamini and Yekutieli \(2005\)](#). In the problem setup described above, these would be calculated as $y_i \pm z_{\beta/2}$ where $\beta = \frac{|\mathcal{R}|\alpha}{n}$. However, we know of no methodology for aggregating the individual CIs to form a single CI that will cover $\bar{\mu}$.

An alternative approach for selective inference is to compute a p -value for testing each y_i , and then mask the p -value as proposed by the AdaPT ([Lei and Fithian \(2018\)](#)) and STAR ([Lei et al. \(2020\)](#)) procedures. These interactive methods allow the data analyst to iteratively build a rejection set in a data adaptive way. A drawback of these approaches, however, is that they only are designed to work with a p -value. In contrast to the BH procedure, there is no available method to cover either the individual signals μ_i or $\bar{\mu}$. Data fission offers one possible path forward:

1. Draw $z_i \sim N(0, \sigma^2)$ and let $f(y_i) = y_i + \tau z_i$ with $g(y_i) = y_i - \frac{1}{\tau} z_i$.
2. Use $f(y_i)$ to select a rejection set of suspected non-nulls using any desired error-control procedure (say AdaPT, STAR or BH).

3. After selecting hypotheses, we can form CIs to cover each $\mu_i \in \mathcal{R}$ with $1 - \alpha$ coverage as

$$g(y_i) \pm z_{\alpha/2} \sigma \sqrt{1 + \frac{1}{\tau^2}} \text{ or we can form a } 1 - \alpha \text{ CI to cover } \bar{\mu} \text{ as } \frac{\sum_{i \in \mathcal{R}} g(y_i)}{|\mathcal{R}|} \pm z_{\alpha/2} \sigma \sqrt{\frac{1 + \frac{1}{\tau^2}}{|\mathcal{R}|}}.$$

To illustrate this procedure, we repeat the experiments in Section 4.3 of [Lei et al. \(2020\)](#) but with fissioned data. Specifically, we let the data be arranged on a grid with non-nulls arranged in a circle in the center with $\mu_i = 2$ for each non-null and $\mu_i = 0$ for each null. We then form a rejection set using the BH, AdaPT, and STAR procedures and compute confidence intervals for $\bar{\mu}$. Results are available in [Figure 4](#). Fissioning the data allows the analyst to form CIs after forming a rejection set by varying τ , while post-selective CIs for non-fissioned data do not have proper coverage. For a more detailed discussion of the simulation and for additional demonstrations on Poisson data, consult [Appendix E.1](#).

4 Application: selective CIs in fixed-design linear regression

We now turn to applying data fission to fixed-design Gaussian linear regression. We expand on the discussion in [Rasines and Young \(2021\)](#), and later build on several results in this section in our treatment of trend filtering in [Section 6](#). We assume that y_i is the dependent variable and $x_i \in \mathbb{R}^p$ is a vector of p features for $i = 1, \dots, n$ samples. For simplicity, we also denote $X = (x_1, \dots, x_n)^T$ as the model design matrix and $Y = (y_1, \dots, y_n)^T$ with:

$$Y = \mu + \epsilon \text{ with } \epsilon = (\epsilon_1, \dots, \epsilon_n)^T \sim N(0, \Sigma),$$

where $\mu = \mathbb{E}[Y|X] \in \mathbb{R}^n$ is a fixed unknown quantity and $\epsilon \in \mathbb{R}^n$ is a random quantity with a known covariance matrix Σ (such as $\sigma^2 I_n$ for known σ ; we discuss unknown σ later).

During the fission phase, we introduce the independent quantities $f(Y)$ and $g(Y)$ created by adding Gaussian noise $Z \sim N(0, \Sigma)$ as described in [Section 2.2](#), letting $f(Y) = Y + \tau Z$, and $g(Y) = Y - \frac{1}{\tau} Z$. We use $f(Y)$ to select a model $M \subseteq [p]$ that, in turn, defines a model design matrix X_M which is a submatrix of X . After selecting M , we then use $g(Y)$ for inference by fitting a linear regression on $g(Y)$ against the selected covariates X_M . However, in an assumption-lean setting where $\mu = \mathbb{E}[Y|X]$ is not guaranteed to be a linear combination of the chosen covariates, it is not clear what the fitted coefficients and corresponding CIs represent. For our purposes, we will use the same problem setup of [Buja et al. \(2019\)](#), but with one significant modification. The above paper focuses on the *random-X* setting where (x_i, y_i) are sampled as random pairs from a common joint density. In the context of data fission, it is only possible to make such an assumption during the fission stage. When conducting inference, X has already been observed once during model selection so we necessarily must condition on the realized values of X . This restricts us to a *fixed-X* setting during the inference stage.

Let $\hat{\beta}$ (as a function of the chosen model M) be defined in the usual way as

$$\hat{\beta}(M) = \underset{\tilde{\beta}}{\operatorname{argmin}} \left\| g(Y) - X_M \tilde{\beta} \right\|^2 = (X_M^T X_M)^{-1} X_M^T g(Y). \quad (3)$$

Our target parameter is then denoted as

$$\beta^*(M) = \underset{\tilde{\beta}}{\operatorname{argmin}} \mathbb{E} \left[\left\| Y - X_M \tilde{\beta} \right\|^2 \right] = (X_M^T X_M)^{-1} X_M^T \mu. \quad (4)$$

We are then able to form CIs that guarantee $1 - \alpha$ coverage of $\beta^*(M)$ as follows.

Theorem 2. For $\hat{\beta}(M)$ from (3) and $\beta^*(M)$ from (4), we have

$$\hat{\beta}(M) \sim N(\beta^*(M), (1 + \tau^{-2})(X_M^T X_M)^{-1} X_M^T \Sigma X_M (X_M^T X_M)^{-1}).$$

Furthermore, we can form a $1 - \alpha$ CI for the k th element of $\beta^*(M)$ as

$$\hat{\beta}^k(M) \pm z_{\alpha/2} \sqrt{(1 + \tau^{-2}) \left[(X_M^T X_M)^{-1} X_M^T \Sigma X_M (X_M^T X_M)^{-1} \right]_{kk}}.$$

A key assumption of this procedure is that the variance is known in order to do the initial split between $f(Y)$ and $g(Y)$ during the fission phase. In the case of unknown variance, one can use an estimator $\hat{\sigma}$ to create the split, but this forces the analyst to then condition on *both* $f(Y)$ and $\hat{\sigma}$, which may not have a tractable distribution in high dimensional settings. In the case where p is fixed and $n \rightarrow \infty$, we explore an extension of this methodology to account for unknown variance in [Section A.4](#). Extending this approach to finite samples and high-dimensional regimes remains an open question for future lines of research.

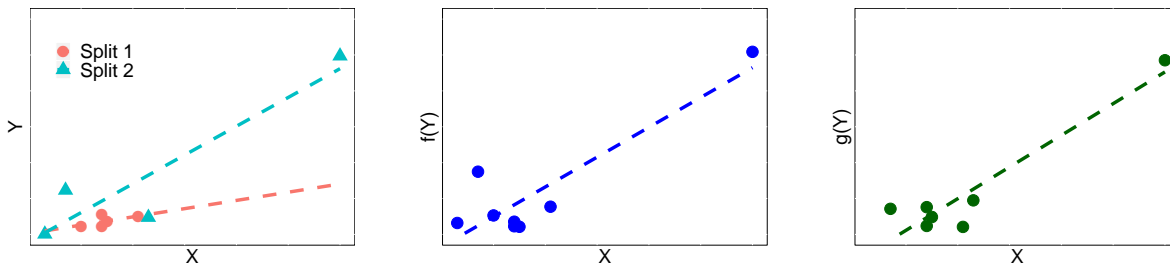


Figure 5. Comparison of data splitting (left) and data fission (middle, right) for dataset with one highly influential point. Splitting the data and fitting a regression results in substantially different fitted models when using data splitting because the fitted values are heavily influenced by a single data point. In contrast, data fission keeps the same X location for every data point, but randomly perturbs the response Y with random noise to create new variables $f(Y)$ and $g(Y)$: notice the slight difference in the two figures. This enables the analyst to keep a “piece” of every data point in both $f(Y)$ and $g(Y)$, ensuring that influential and leverage points have an impact in both copies of the dataset.

A key advantage that data fission has over data splitting is that it allows the analyst to smoothly trade off information between selection and inference datasets by tuning τ , while data splitting forces the analyst to allocate points discretely to either the selection or inference datasets. When the sample size is large and the distribution of covariates is well behaved, data splitting may be able to tradeoff information relatively smoothly by changing the proportion of data points in each sample. However, data fission will outperform data splitting in settings with small sample size with a handful of points with high leverage. Data splitting has a disadvantage in this setting because the analyst is forced to choose to allocate each of these leverage points to either the selection or inference dataset. In contrast, data fission enables the analyst to “hedge their bets” so that a piece of the information contained in each leverage point is allocated to both the selection and inference datasets. Figure 5 offers an illustration of this tendency on an example dataset and an extended discussion on this topic can be found in Appendix C.

We now demonstrate the advantages that data fission has over data splitting through an empirical study. We conduct inference on some vector Y given a set of covariates X and a known covariance matrix $\Sigma = \sigma^2 I_n$ as follows:

1. Decompose y_i into $f(y_i) = y_i - Z_i$ and $g(y_i) = y_i + Z_i$ where $Z_i \sim N(0, \sigma^2)$.
2. Fit $f(y_i)$ using LASSO to select features, denoted as $M \subseteq [p]$.¹
3. Fit $g(y_i)$ by linear regression without regularization using only the selected features
4. Construct CIs for the coefficients trained in step 3, each at level α , using Theorem 2.

Simulation setup. We choose $\sigma^2 = 1$ and generate $n = 16$ data points with $p = 20$ covariates. For the first 15 data points, we have an associated vector of covariates $x_i \in \mathbb{R}^p$ generated from independent Gaussians. The last data point, which we denote x_{lev} , is generated in such a way as to ensure it is likely to be more influential than the remaining observations due to having much larger leverage. We define $x_{\text{lev}} = \gamma(|X_1|_\infty, \dots, |X_p|_\infty)$ where X_k denotes the k -th column vector of the model design matrix X formed from the first 15 data points and γ is a parameter that we will vary within these simulations that reflects the degree to which the last data point has higher leverage than the first set of data points. We then construct $y_i \sim N(\beta^T x_i, \sigma^2)$. The parameter β is nonzero for 4 features: $(\beta_1, \beta_{16}, \beta_{17}, \beta_{18}) = S_\Delta(1, 1, -1, 1)$ where S_Δ encodes the signal strength.

¹In our experiments, we use `cv.glmnet` in R package `glmnet` and choosing the tuning parameter λ by the 1 standard deviation rule, which can be found in the value of `lambda.1se`

We use 500 repetitions and summarize performance as follows. For the selection stage, we compute the power and precision of selecting features with a nonzero parameter:

$$\text{power}^{\text{selected}} := \frac{|j \in M : \beta_j \neq 0|}{|j \in [p] : \beta_j \neq 0|}, \text{ and } \text{precision}^{\text{selected}} := \frac{|j \in M : \beta_j \neq 0|}{|M|}. \quad (5)$$

For inference, we use the false coverage rate and mean CI length within the selected model:

$$\text{FCR} := \frac{|k \in M : [\beta^*(M)]_k \notin \text{CI}_k|}{\max\{|M|, 1\}}, \text{ Avg. CI Length} := \frac{1}{|M|} \sum_{k \in M} |\text{CI}_k(2) - \text{CI}_k(1)|, \quad (6)$$

where CI_k is the CI for $[\beta^*(M)]_k$ and $\text{CI}_k(1)$, $\text{CI}_k(2)$ are the lower and upper bound of CI_k .

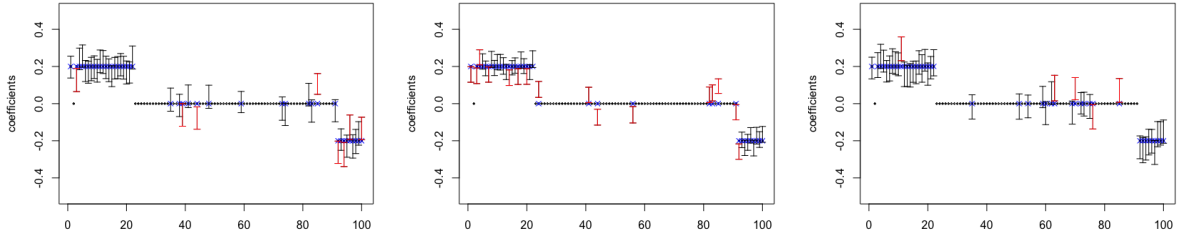


Figure 6. An instance of the selected feature (blue crosses) and the constructed CIs using fissioned data (left), full data twice (middle), and split data (right) with $S_\Delta = 0.2$ and target FCR set at 0.2. The selected features are marked by blue crosses, which include all of the nonzero coefficients (corresponding to almost 100% power for selection) and also a few zero coefficients (corresponding to around 70% precision for selection). CIs which do not cover the parameters correctly are marked red.

As an illustration, [Figure 6](#) shows an instance of the selected features and corresponding CIs for an example trial run. As a point of comparison, we compare the CIs constructed using data fission with those constructed using data splitting (when 50% of the dataset is used for selection and the remaining for inference). We also compare these results to the (invalid) procedure where the original dependent variable is used twice to both select features and construct intervals (replacing $f(y_i)$ and $g(y_i)$ both by y_i in the above algorithm). The third methodology will not have coverage guarantees but it is still a useful point of comparison for evaluating the performance of the other two (valid) methodologies.

[Figure 7](#) shows results averaged over 500 trials. Data splitting and data fission both control the FCR, but data fission dominates data splitting across every other metric—including significantly tighter CIs and higher power and precision. In simulation studies with larger sample sizes and less skewed covariates, data fission and data splitting have comparable performance—see [Appendix E.2](#) for details.

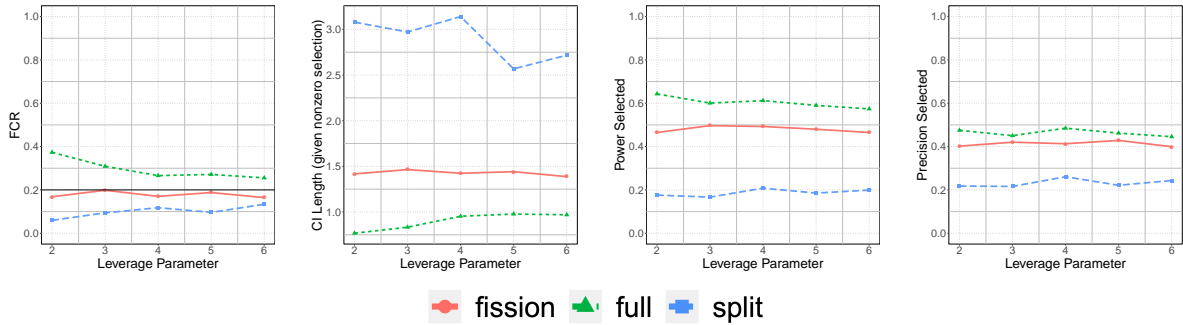


Figure 7. FCR, average length of the CIs, and power/precision for the selected features, when varying the leverage parameter γ in $\{2, 3, 4, 5, 6\}$. The results are averaged over 500 trials. Both data splitting and data fission still control FCR, but data fission now has higher power and precision, as well as tighter CIs than data splitting.

5 Application to selective CIs in fixed-design generalized linear models and other quasi-MLE problems

For regression problems involving non-Gaussian distributed data, the same generic principle can be used as in [Section 4](#). If the underlying distribution of Y is known up to a set of unknown parameters and aligns with one of the distributions described in [Appendix B](#), we can fission the data and then use $f(Y)$ for selection, while reserving $g(Y)|f(Y)$ to conduct inference. Even in cases where we are certain that the distribution of Y has been properly specified and the fission procedure is valid, it is important to construct CIs that are robust to model misspecification for two reasons. First, because it is unlikely in practical settings that we are going to be able to select a set of covariates that corresponds to the “actual” conditional mean of the data. Second, the post-selective distribution $f(Y)|g(Y)$ may be ill-behaved and difficult to work with even if Y is easy to model. For example, if $Y \sim \text{Ber}(\theta)$, the post-selective distribution $g(Y)|f(Y)$ constructed from [Section 4](#) is $\text{Ber}\left(\frac{\theta}{\theta + (1-\theta)[p/(1-p)]^{2f(Y)-1}}\right)$. Maximizing this likelihood function will be challenging since the likelihood is non-convex, so it may be practical to model the likelihood as a probit or logistic model as a working assumption.

This approach of using maximum likelihood estimation to train a model but to construct guarantees in an assumption-lean setting is termed quasi-maximum likelihood estimation (QMLE). Most work in this setting, such as [Huber \(1967\)](#), [Buja et al. \(2019\)](#), and [Rinaldo et al. \(2019\)](#), are designed around a background assumption where both the covariates and response are treated as i.i.d. random variables. Such theory is inapplicable to data fission since the covariates are observed during the model selection stage and therefore inference on $g(Y)$ is only valid if both X and $f(Y)$ are conditioned on. [Fahrmeir \(1990\)](#), however, works in the setting of non-identically distributed but independent data with fixed covariates and therefore can be applied to this setting. We first recap the relevant theory and then apply it to data fission when used for forming post-selective CIs in GLMs.

5.1 Problem setup and a recap of QMLE methods

Suppose we observe n random observations $y_i \in \mathbb{R}$ alongside fixed covariates $x_i \in \mathbb{R}^p$ and that we fission each data point into $f(y_i)$ and g_i such that the following assumption holds.

Assumption 1. *Data fission is conducted such that $g(y_i) \perp g(y_k)|f(Y), X$ for all $i \neq k$.*

This is a different condition compared to the rules described in [Section 1](#). Any fissioning rule which satisfies **(P1)** would also satisfy this (weaker) condition. The majority of decompositions in [Appendix B](#) following **(P2)** also satisfy [Assumption 1](#) but this is not necessarily the case — for instance,

the third rule for fissioning Gaussian distributed data would result in a post-selective distribution that is tractable but with correlated entries. However, if a fissioning process exists that creates independent entries in $g(Y)|f(Y), X$, the procedures outlined in this section will apply.

During model selection, a model $M \subseteq [p]$ is chosen from $f(Y)$ which result in an annealed set of covariates $\tilde{x}_i \in \mathbb{R}^{|M|}$ and model design matrix X_M . We then find an estimate for β using a working model of the density for $g(y_i)|f(Y), X$ as $p(g(y_i)|\beta, f(Y), X_M)$, which defines the quasi-likelihood function $L_n(\beta) := \sum_{i=1}^n \log p(g(y_i)|\beta, f(Y), X_M)$. Denote the score function $s_n(\beta) = \frac{\partial L_n}{\partial \beta}$ as well as the quantities $H_n(\beta) = -\frac{\partial^2 L_n}{\partial \beta \partial \beta^T}$, and $V_n(\beta) = \text{Var}(s_n(\beta))$. If $\mathbb{E}(H_n(\beta))$ is positive definite, the target parameter $\beta^*(M)$ is the root of $E(s_n(\beta))$ which is also the parameter which minimizes the KL distance between the true distribution (denoted as $q(g(y_i)|f(Y), X)$) and the working model because

$$\begin{aligned} \beta_n^*(M) &= \underset{\beta}{\operatorname{argmin}} \mathbb{E}(\log q(g(y_i)|X, f(Y)) - L_n(\beta)) \\ &= \underset{\beta}{\operatorname{argmin}} D_{KL} \left(\prod_{i=1}^n q(g(y_i)|X, f(Y)) \parallel \prod_{i=1}^n p(g(y_i)|\beta, f(Y), X_M) \right). \end{aligned}$$

We define $\hat{\beta}_n(M)$ as the quasi-likelihood maximizer. Under mild regularity conditions, $\hat{\beta}_n(M)$ behaves asymptotically like $N(\beta^*(M), H_n^{-1}(\beta_n^*(M))V_n(\beta_n^*(M))H_n^{-1}(\beta_n^*(M)))$. Plug-in estimates $\hat{H}_n := H_n(\hat{\beta}_n(M))$ and $\hat{V}_n := s_n(\hat{\beta}_n(M))s_n(\hat{\beta}_n(M))^T$ will yield asymptotically conservative estimates for the covariance matrix, allowing the user to form confidence intervals. For a detailed technical account, see Appendix A.5.

5.2 Simulation results

We verify the efficacy of this procedure through an empirical simulation. The advantages of data fission are again most apparent in settings with relatively few data points and a handful of leverage points just as we saw in the Gaussian case in Section 4.

Simulation setup. Let y_i be the dependent variable with $y_i \sim \text{Pois}(\exp\{\beta^T x_i\})$ where $x_i \in \mathbb{R}^p$ is a vector of p features. We generate $n = 16$ data points with $p = 20$ covariates, where the parameter β is nonzero for 4 features: $(\beta_1, \beta_{16}, \dots, \beta_{19}) = S_\Delta(1, 1, -1, 1)$ and S_Δ encodes the signal strength. For the first 15 observations, $x_i \in \{0, 1\}^2 \times \mathbb{R}^{18}$, where the first two follow $\text{Ber}(1/2)$ and the rest follow independent standard Gaussians. The last data point, which we again denote $x_{\text{lev}} = \gamma(|X_1|_\infty, \dots, |X_p|_\infty)$ where X_k denotes the k -th column vector of the model design matrix X formed from the first 15 data points and γ is the leverage parameter. Our proposed procedure is:

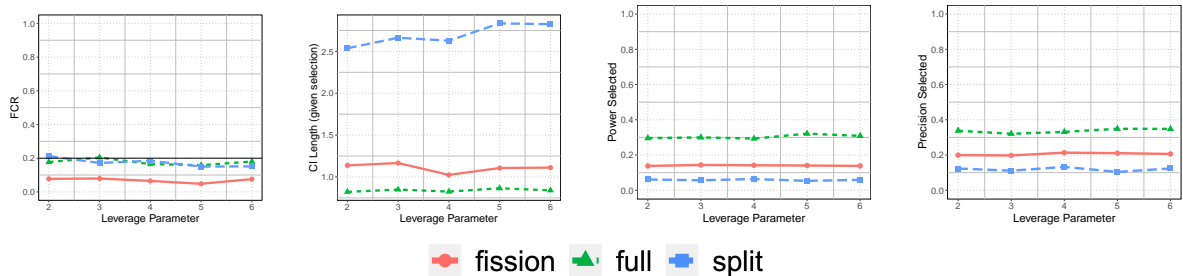


Figure 8. FCR, length of the CIs, FSR, power for the sign of parameters, and power and precision for the selected features, when varying the leverage parameter α in $\{2, 3, 4, 5, 6\}$ for Poisson data over 500 trials. CIs constructed using data fission are tighter than data splitting, and power during the selection stage is higher..

1. Decompose each y_i as $f(y_i) \sim \text{Bin}(y_i, 0)$, and $g(y_i) = y_i - f(y_i)$.
2. Fit $f(y_i)$ by the GLM with log-link and LASSO regularization to select $M \in [p]$.²
3. Fit $g(y_i)$ by another GLM without regularization with log-link using *only* the selected features and an offset of $\log(1 - p)$ to account for the effect of the randomization.
4. Construct CIs for the coefficients trained in the third step, each at level α and with the standard errors estimated as in [Theorem 5](#). For the experiments shown below, we also apply a finite sample correction as described in [Pustejovsky and Tipton \(2018\)](#).

Since step 2 may not select the correct model, the CIs in step 4 cover $\beta_n^*(M)$.

Results are shown in [Figure 8](#). Model performance metrics are the same as those used in [Section 4](#) with $\beta_n^*(M)$ replacing $\beta^*(M)$. The CIs constructed with each method control the FCR empirically in this particular case, but the CI lengths for data fission are significantly tighter than for data splitting. Data fission is also more powerful at the selection stage than data splitting. Results for higher n settings can be found in [Appendix E.2](#). In these cases, using the full dataset twice no longer results in FCR control, as expected. Interestingly, unlike in the Gaussian regression case, data fission results in tighter confidence intervals than data splitting for large n settings as well.

6 Application to post-selection inference for trend filtering and other nonparametric regression problems

Consider a nonparametric setup with y_i and covariates x_i following $y_i = f_0(x_i) + \epsilon_i$, where f_0 is the underlying function to be estimated and ϵ_i is random noise. We denote $Y = (y_1, \dots, y_n)^T$ and $\epsilon = (\epsilon_1, \dots, \epsilon_n)^T$. For now, assume that $\epsilon \sim N(0, \Sigma)$ for some known Σ . We can apply the methodologies of [Section 2.2](#) and [Section 4](#) to this problem as follows:

1. Decompose Y into $f(Y) = Y + \tau Z$ and $g(Y) = Y - \frac{1}{\tau} Z$ where $Z \sim N(0, \Sigma)$.
2. Use $f(X)$ to choose a basis a_1, \dots, a_p for the series expansion of x_i and denote $a(x_i) = (a_1(x_i), \dots, a_p(x_i))^T$. Let A denote the matrix of basis vectors for all n data points.
3. Use $g(X)|f(X)$ to construct pointwise or uniform CIs as described below.

Pointwise CI. We first note that the fitted line

$$\hat{\beta}(A) = \underset{\beta}{\operatorname{argmin}} \|g(Y) - A\beta\|^2 = (A^T A)^{-1} A^T g(Y) \quad (7)$$

corresponds to $A\hat{\beta}(A)$ which is just the projection of $g(Y)$ onto the basis chosen during the model selection stage. Meanwhile, we define the *projected regression function* as

$$\beta^*(A) = \underset{\beta}{\operatorname{argmin}} \mathbb{E} \left[\|Y - A\beta\|^2 \right] = (A^T A)^{-1} A^T f_0(X). \quad (8)$$

We are then interested in using the fitted estimates $\hat{\mu}_{x_i}(A) = a(x_i)^T \hat{\beta}(A)$ to construct intervals that guarantee coverage for the underlying function $f_0(x_i)$ projected onto the chosen basis which we denote as $\mu_{x_i}^*(A) = a(x_i)^T \beta^*(A)$ and refer to as the *projected mean*.

²In our examples, we use `cv.glmnet` in the R package `glmnet` and choose the tuning parameter λ by the 1 standard deviation rule, which can be found in the value of `lambda.1se`

Corollary 1. Recall the definitions of $y_i, \epsilon_i, \hat{\beta}(A), \beta^*(A)$ from (7) and (8). When ϵ has known variance Σ , $\hat{\mu}_{x_i}(A) \sim N(\mu_{x_i}^*(A), (1 + \tau^{-2})a(x_i)^T(A^T A)^{-1}A^T \Sigma A(A^T A)^{-1}a(x_i))$ and a $1 - \alpha$ CI for $\mu_{x_i}^*(A)$ is $\hat{\mu}_{x_i}(A) \pm z_{\alpha/2} \sqrt{(1 + \tau^{-2})a(x_i)^T(A^T A)^{-1}A^T \Sigma A(A^T A)^{-1}a(x_i)}$.

Uniformly valid CIs. We can also construct uniformly valid CIs $\{CI_i\}_{i=1}^n$ to cover the projected mean, controlling the *simultaneous* type I error rate defined as $\mathbb{P}(\exists i \in [n] : \mu_{x_i}^*(A) \notin CI_i)$. Here, we further assume homoscedastic errors so $\Sigma = \sigma^2 I_n$. Construct $CI_i := (\hat{\mu}_{x_i}(A) - w, \hat{\mu}_{x_i}(A) + w)$, where the width $w := c(\alpha) \cdot \sigma \sqrt{(1 + \tau^{-2})a(x_i)^T(A^T A)^{-1}a(x_i)}$, where $c(\alpha)$ is a multiplier. By Eq. (5.5) in [Koenker \(2011\)](#), $c(\alpha)$ is the solution to the equation $\frac{|\gamma|}{2\pi} e^{-c^2/2} + 1 - \Phi(c) = \alpha/2$, where $|\gamma| = \sum_{i=1}^{n-1} \|\tilde{a}(x_{i+1}) - \tilde{a}(x_i)\|_2$ is the length of the curve connected by $\tilde{a}(x_i) := \frac{(A^T A)^{-1/2} a(x_i)}{\|(A^T A)^{-1/2} a(x_i)\|}$.

Fact 1 ([Koenker \(2011\)](#)). The above constructed CIs will cover the projected mean uniformly: $\mathbb{P}(\exists i \in [n] : \mu_{x_i}^*(A) \notin CI_i) \leq \alpha$, where $\{\mu_{x_i}^*(A)\}_{i=1}^n$ denotes the projected mean.

6.1 Application to trend filtering

We explore how this approach to nonparametric inference performs empirically through the lens of *trend filtering* as proposed by [Kim et al. \(2009\)](#) and [Steidl et al. \(2006\)](#). Here, we consider the problem of estimating the underlying smooth trend of a time series $y_t \in \mathbb{R}$ with $t = 1, \dots, n$. We have the same equation as in the standard nonparametric setup, but with $x_i = t$ for all i and thus have that $y_t = f_0(t) + \epsilon_t$. Our goal is to estimate the underlying trend $(f_0(1), \dots, f_0(n))$. The approach of (first order) trend filtering is to fit a piecewise linear approximation to this data with adaptively chosen breakpoints or *knots* by solving: $\hat{x} = \operatorname{argmin}_{x_t \in \mathbb{R}} 1/2 \sum_{t=1}^n (y_t - x_t)^2 + \lambda \sum_{t=2}^{n-1} |x_{t-1} - 2x_t + x_{t+1}|$. Although we focus on first order trend filtering, our methodology straightforwardly generalizes to higher order trend filtering. For a detailed overview of trend filtering, including generalization to higher order polynomials, see [Appendix D](#).

A key issue with trend filtering is that parametric uncertainty quantification is not generally tractable even when strong distributional assumptions are made since the knots are chosen adaptively. In some settings, data carving approaches may offer a viable path forward. When the (fused or generalized) lasso is used to select the choice of knots, methods such as [Chen et al. \(2022\)](#), [Duy and Takeuchi \(2021\)](#), and [Hyun et al. \(2018\)](#) can be used to construct tests and CIs with valid post-selective distributions. The drawback of these approaches is that they offer the analyst no flexibility during the selection stage. If the analyst wishes to change the degree of the fitted polynomial or decrease the number of chosen knots after seeing preliminary results, inferential guarantees are no longer available. Although such actions are common in applied data analysis, data carving approaches do not easily handle these sorts of ad-hoc changes to the prespecified selection methodology. Data fission offers an alternative path forward which offers the analyst flexibility to change the amount of regularization (alter the number of knots) or change the degree of the trend filtered estimate after a preliminary view of the selected model performance.

Similar to [Section 4](#), an assumption of known variance is required when using data fission in order to ensure the selection and inference datasets are independent. Approaches that estimate variance empirically are explored in [Appendix E.5.3](#) but we leave theoretical guarantees for future work. The proposed procedure is:

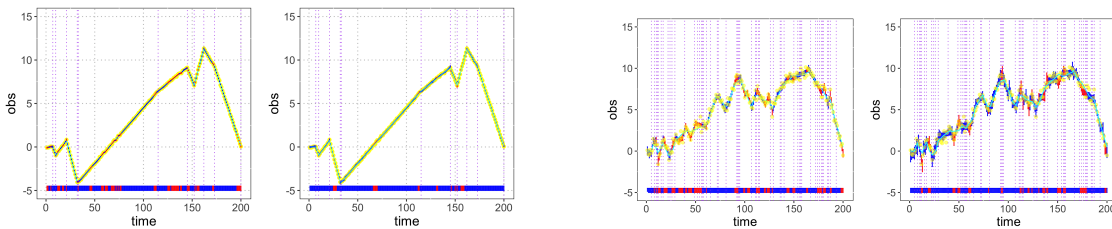
1. Decompose Y into $f(Y) = Y + \tau Z$, $g(Y) = Y - \frac{1}{\tau} Z$ where $Z \sim N(0, \Sigma)$
2. Train a k -th order trendfilter using $f(Y)$ and select the tuning parameter λ by selecting the set of knots $\{\tau_k\}_{k \in 1}^m$ with the minimum cross-validation error.³

³Although we restrict ourselves to a fixed selection rule for simulation purposes, data fission allows for the use of any arbitrary method of choosing the set of knots. For a discussion of alternative methods for choosing the tuning parameter λ , see [Appendix E.5.4](#).

3. Construct a k th degree falling factorial basis, as described in Tibshirani (2014), with knots at $\{\tau_k\}_{k=1}^m$ and use this to regress against $g(Y)$. Note that when $k = 0$ or $k = 1$, this reduces to generating the more familiar truncated power basis.
4. Get *pointwise* CIs for each data point $t = 1, \dots, n$ at level α as described in Corollary 1. In cases where $\Sigma = \sigma^2 I_n$, we can also construct *uniform* CIs using Fact 1.

We verify the efficacy of this approach through an experiment.

Simulation setup. We simulate data as $y_t = f(t) + z_t$ for $t \in [n]$, where $z_t \sim N(0, \sigma^2)$, and $f_0(t)$ is generated by $f_0(t+1) = f_0(t) + v_t$. With probability $1 - p$, we let $v_{t+1} = v_t$ (no slope change in the trend). With probability p , we choose v_{t+1} from a uniform distribution on $[-0.5, 0.5]$. We choose the initial slope $v_1 \sim \text{Unif}[-0.5, 0.5]$ and set $f_0(0) = 0$.



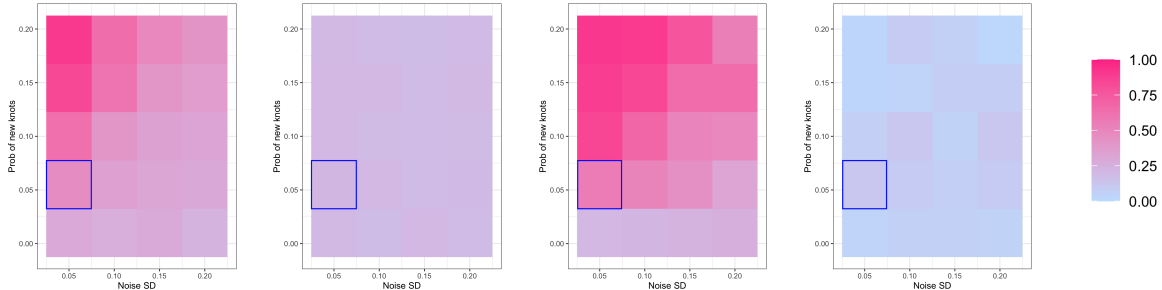
(a) Dataset generated with smaller noise ($\sigma = 0.05$) and low probability of new knots ($p = 0.05$). Target FCR equals 0.2 with empirical coverage of 0.1 for data fission and 0.285 when using the full dataset twice.

(b) Dataset generated with larger noise ($\sigma = 0.5$) and higher probability of new knots ($p = 0.3$). Target FCR equals 0.2 with empirical coverage of 0.225 for data fission and 0.365 when using the full dataset twice.

Figure 9. Two instances of the observed points (in yellow) and the *pointwise* CIs (in blue if correctly cover the trend, in red if not; the time points with false coverage is also amplified in the bar at the bottom) using two types of methods: full data twice (left), and data fission (right). The underlying projected mean is marked in cyan, which mostly overlaps with the true underlying trend. The true knots are marked by vertical lines. Using data fission results in correct empirical coverage (the 0.225 above was for just one run, the average is below 0.2). In contrast, the FCR is not controlled when using the full dataset twice; it worsens as the underlying noise and trend become more volatile.

We use the above procedure to select knots and conduct inference. An example of how this methodology performs when compared to the (invalid) approach of using the full dataset twice is shown in Figure 9 for *pointwise* CIs. As there is not an obvious way to apply data splitting to trend filtering, this view is excluded from our comparison. Although using the full dataset twice is invalid, it performs worse for datasets that are more volatile, either in terms of the underlying structural trend (i.e. more knots and/or larger slopes) or in terms of the underlying noise level. For a similar demonstration of how uniform CIs perform for a single example run, see Appendix E.5.2.

We repeat over 500 trials and report the results in Figure 10. Reusing the full dataset performs most comparably to data fission when the noise is small and the probability of new knots is low. For noisier data and more volatile trends, reusing the confidence intervals results in anticonservative CIs. See Appendix E.5 for more detailed empirical results.



(a) FCR using full data twice (b) FCR using data fission (c) Simult. type I error (double dip) (d) Simult. type I error (fission)

Figure 10. FCR for the **pointwise CIs** and simultaneous type I error for **uniform CIs** when varying the probability of having knots p in $\{0.01, 0.55, 0.1, 0.145, 0.19\}$ and the noise SD in $\{0.05, 0.1, 0.15, 0.2\}$ (the blue circled cell represents the setting for the first shown instance in Figure 9). The CIs generated using full data twice do not have valid FCR or simultaneous type I error control, especially when p is large (more knots) and the noise standard deviation is small, but data fission is always valid.

6.2 Application to spectroscopy

We demonstrate this methodology on an example in observational astronomy. In Politsch et al. (2020b), the authors introduce trend filtering as a tool for astronomical data analysis because of settings within astronomy where a step in the analysis pipeline reduces to one dimensional data compression. One example is the use of trend filtering to aid in spectral classification. Here, astronomers observe a spectrum consisting of wavelengths (λ) and measurements of the coadded flux ($f(\lambda)$) at each wavelength for an object of interest. Trend filtering is then used to create a “spectral template”—a smoothed line of best fit for the observed spectrum. This template is combined with emission-line parameter estimates to classify the astronomical object. The authors demonstrate that trend filtering performs well empirically compared to the existing state-of-the-art for creating spectral templates which revolve around low-dimensional principal component analysis. We use this analysis as a way of demonstrating how CIs constructed using data fission appear for real data.

The dataset used for this analysis is the twelfth data release of the Baryon Oscillation Spectroscopic Survey (Alam et al. (2015)). We estimate a smoothed line of best fit using trend filtering, along with pointwise and uniform confidence bands (using the methods from Section 6) designed to cover the conditional mean $\mu = \mathbb{E}[f(\lambda)|\lambda]$ of the observed spectra of the same three objects⁴ discussed in Politsch et al. (2020b). In this setting, the flux measurement variances are known a priori as they are constructed from the BOSS spectroscopy pipeline (Bolton et al. (2012)) and account for the statistical uncertainty introduced by photon noise, CCD read noise, and sky-subtraction error. The results are shown in Figure 11 for the quasar and in Appendix F for the remaining objects. Since the confidence bands displayed are covering the conditional mean and *not* the observed data, there is no objective “ground truth” to compare the outputs of the model to in order to assess goodness of fit. Therefore, the results need to be judged holistically.

⁴(A) A **quasar**. DR12, Plate = 7130, MJD = 5659, Fiber = 58. Located at (RA,Dec, z) \approx (349.737°, 33.414°, 2.399); (B) A **galaxy**. DR12, Plate = 7140, MJD = 56569, Fiber = 68. Located at (RA,Dec, z) \approx (349.374°, 33.617°, 0.138); (C) A **star**. DR12, Plate = 4055, MJD = 55359, Fiber = 84. Located at (RA,Dec, z) \approx (236.834°, 0.680°, 0.000).

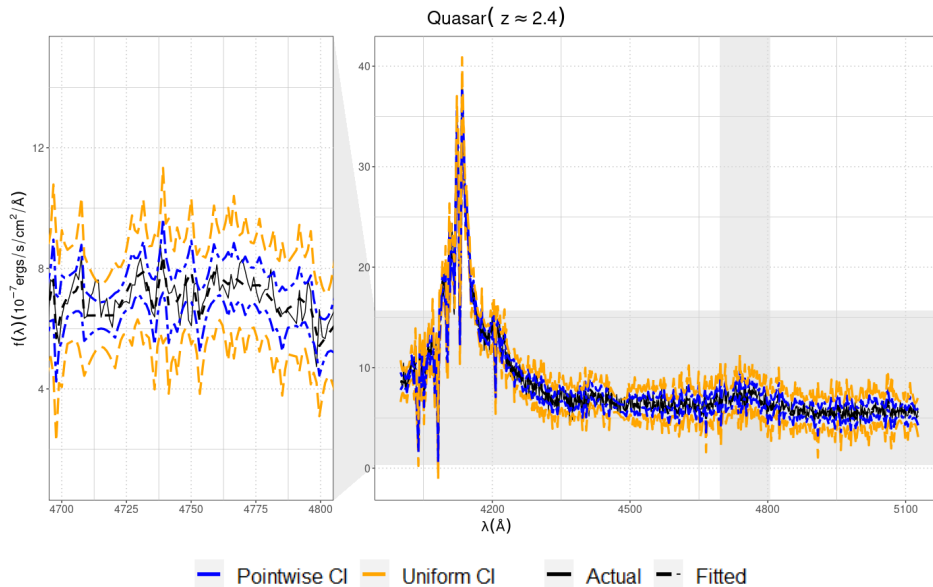


Figure 11. Fitted values as well as uniform and pointwise CIs for the quasar object fit using linear trend filtering. The right view shows the trend filter over the entire spectrum, but the left view “zooms in” on a smaller subset of the data to aid in visual identification.

7 Conclusion

We have proposed a method for selective inference through external randomization that allows flexibility to choose models in an arbitrary and data dependent way, like in data splitting, but also provides a more efficient split of available information in some settings. We demonstrate the efficacy of these methods in four applications: effect size estimation after interactive multiple testing, Gaussian linear regression, generalized linear models, and trend filtering. In the case of linear regression and GLMs, we note tighter CIs and higher power compared to data splitting in settings with leverage points and small sample size. For trend filtering, data fission enables uncertainty quantification while offering flexibility in choosing the number of knots and degree of the polynomial based on heuristic criteria.

Numerous avenues for follow-up work exist. Although we note promising empirical results that suggest this procedure can be generalized to situations where the variance is unknown in fixed dimensional settings, additional work needs to be done to establish guarantees in high dimensional settings. Independently, it is possible to repeat the data fission procedure multiple times in parallel, but aggregating results seems nontrivial. Last, we anticipate applications to contemporary problems such as the creation of fake datasets and enabling differential privacy (beyond the Gaussian mechanism).

Acknowledgements. We thank Collin Politsch for help with the data for [Section 6.2](#) and Anna Neufeld for discovering a mistake in the original version of the manuscript.

References

- Alam, S., F. D. Albareti, C. A. Prieto, F. Anders, S. F. Anderson, T. Anderton, B. H. Andrews, E. Armengaud, E. Aubourg, S. Bailey, and et al. (2015). The eleventh and twelfth data releases of the Sloan digital sky survey: final data from SDSS-III. *The Astrophysical Journal Supplement Series* 219(1).
- Barber, R. F. and E. J. Candès (2015). Controlling the false discovery rate via knockoffs. *The Annals of Statistics* 43(5), 2055 – 2085.

- Benjamini, Y. and Y. Hochberg (1995). Controlling the false discovery rate: A practical and powerful approach to multiple testing. *J. of the Royal Stat. Soc.: Series B* 57(1), 289–300.
- Benjamini, Y. and D. Yekutieli (2005). False discovery rate-adjusted multiple confidence intervals for selected parameters. *J. of the Amer. Stat. Assoc.* 100(469), 71–81.
- Bolton, A., D. Schlegel, E. Aubourg, S. Bailey, V. Bhardwaj, J. Brownstein, S. Burles, Y.-M. Chen, K. Dawson, D. Eisenstein, J. Gunn, G. Knapp, C. Loomis, R. Lupton, C. Maraston, D. Muna, A. Myers, M. Olmstead, N. Padmanabhan, and W. Wood-Vasey (2012). Spectral classification and redshift measurement for the SDSS-III baryon oscillation spectroscopic survey. *The Astron. J.* 144.
- Brockwell, A. (2007). Universal residuals: A multivariate transformation. *Stat. & Prob. Letters* 77(14), 1473–1478.
- Buja, A., L. Brown, R. Berk, E. George, E. Pitkin, M. Traskin, K. Zhang, and L. Zhao (2019). Models as Approximations I: consequences illustrated with linear regression. *Stat. Sci.* 34(4).
- Buja, A., L. Brown, A. K. Kuchibhotla, R. Berk, E. George, and L. Zhao (2019). Models as approximations II: A model-free theory of parametric regression. *Stat. Sci.* 34(4), 545–565.
- Chen, Y., S. Jewell, and D. Witten (2022). More powerful selective inference for the graph fused lasso. *J. of Comp. and Graph. Stat.* 0(0), 1–11.
- Duy, V. N. L. and I. Takeuchi (2021). Parametric programming approach for more powerful and general lasso selective inference. *arXiv:2004.09749*.
- Fahrmeir, L. (1990). Maximum likelihood estimation in misspecified generalized linear models. *Stat.* 21(4), 487–502.
- Fithian, W., D. Sun, and J. Taylor (2014). Optimal inference after model selection. *arXiv:1410.2597*.
- Huber, P. J. (1967). The behavior of maximum likelihood estimates under nonstandard conditions. In *Proc. of the Fifth Berkeley Symp. on Math. Stat. and Prob.*, Volume 1, pp. 221–233.
- Hyun, S., M. G’Sell, and R. J. Tibshirani (2018). Exact post-selection inference for the generalized lasso path. *Elec. J. of Stat.* 12(1), 1053 – 1097.
- Ignatiadis, N., S. Saha, D. L. Sun, and O. Muralidharan (2021). Empirical Bayes mean estimation with nonparametric errors via order statistic regression on replicated data. *J. of the Amer. Stat. Assoc. (online)*.
- Kim, S.-J., K. Koh, S. Boyd, and D. Gorinevsky (2009). ℓ_1 trend filtering. *SIAM Review* 51(2).
- Koenker, R. (2011). Additive models for quantile regression: Model selection and confidence band-aids. *Brazilian J. of Prob. and Stat.* 25(3), 239–262.
- Last, G. and M. Penrose (2017). *Lectures on the Poisson Process*. Cambridge Univ. Press.
- Lee, J. D., D. L. Sun, Y. Sun, and J. E. Taylor (2016). Exact post-selection inference, with application to the lasso. *The Annals of Stat.* 44(3), 907 – 927.
- Lei, L. and W. Fithian (2018). AdaPT: an interactive procedure for multiple testing with side information. *J. of the Royal Stat. Soc.: Series B* 80(4), 649–679.
- Lei, L., A. Ramdas, and W. Fithian (2020). A general interactive framework for false discovery rate control under structural constraints. *Biometrika* 108(2), 253–267.
- Li, X. and W. Fithian (2021). Whiteout: when do fixed-X knockoffs fail? *arXiv:2107.06388*.

- Mammen, E. and S. van de Geer (1997). Locally adaptive regression splines. *The Annals of Stat.* 25(1), 387 – 413.
- Oliveira, N. L., J. Lei, and R. J. Tibshirani (2021). Unbiased risk estimation in the normal means problem via coupled bootstrap techniques. *arXiv:2109.10451*.
- Politsch, C. A., J. Cisewski-Kehe, R. A. C. Croft, and L. Wasserman (2020a). Trend filtering – I. A modern statistical tool for time-domain astronomy and astronomical spectroscopy. *Monthly Notices of the Royal Astron. Soc.* 492(3), 4005–4018.
- Politsch, C. A., J. Cisewski-Kehe, R. A. C. Croft, and L. Wasserman (2020b). Trend filtering – II. Denoising astronomical signals with varying degrees of smoothness. *Monthly Notices of the Royal Astron. Soc.* 492(3), 4019–4032.
- Pustejovsky, J. E. and E. Tipton (2018). Small-sample methods for cluster-robust variance estimation and hypothesis testing in fixed effects models. *J. of Business & Econ. Stat.* 36(4).
- Ramdas, A. and R. J. Tibshirani (2014). Fast and flexible ADMM algorithms for trend filtering. *J. of Comp. and Graphical Stat.* 25, 839 – 858.
- Rasines, D. G. and G. A. Young (2021). Splitting strategies for post-selection inference. *arXiv:2102.02159*.
- Rinaldo, A., L. Wasserman, and M. G’Sell (2019). Bootstrapping and sample splitting for high-dimensional, assumption-lean inference. *The Annals of Stat.* 47(6), 3438 – 3469.
- Sarkar, S. K. and C. Y. Tang (2021, 12). Adjusting the Benjamini–Hochberg method for controlling the false discovery rate in knockoff-assisted variable selection. *Biometrika*. asab066.
- Steidl, G., S. Didas, and J. Neumann (2006). Splines in higher order TV regularization. *J. of Comp. and Graph. Stat.* 70, 241 – 255.
- Tian, X. and J. Taylor (2017). Asymptotics of selective inference. *Scandinavian J. of Stat.* 44(2).
- Tian, X. and J. Taylor (2018). Selective inference with a randomized response. *The Annals of Stat.* 46(2), 679–710.
- Tibshirani, R., M. Saunders, S. Rosset, J. Zhu, and K. Knight (2005). Sparsity and smoothness via the fused lasso. *J. of the Royal Stat. Soc.: Series B* 67(1), 91–108.
- Tibshirani, R. J. (2014). Adaptive piecewise polynomial estimation via trend filtering. *The Annals of Stat.* 42(1), 285 – 323.
- Tibshirani, R. J., J. Taylor, R. Lockhart, and R. Tibshirani (2016). Exact post-selection inference for sequential regression procedures. *J. of the Amer. Stat. Assoc.* 111(514), 600–620.
- Ulm, K. (1990). Simple method to calculate the confidence interval of a standardized mortality ratio (SMR). *Amer. J. of Epidemiology* 131(2), 373–375.
- White, H. (1980). A heteroskedasticity-consistent covariance matrix estimator and a direct test for heteroskedasticity. *Econometrica* 48(4), 817–838.
- White, H. (1982). Maximum likelihood estimation of misspecified models. *Econometrica* 50(1).
- Xing, X., Z. Zhao, and J. S. Liu (2021). Controlling false discovery rate using Gaussian mirrors. *J. of the Amer. Stat. Assoc. (online)*.

A Proofs and additional theoretical results

A.1 Proof of Theorem 1

Proof. Note that because the density $p(z | x)$ must integrate to 1, we can view the function $H(\theta_1, \theta_2)$ as a normalization factor since

$$H(\theta_1, \theta_2) = \frac{1}{\int_{-\infty}^{\infty} \exp\{\theta_1^T x - \theta_2^T A(x)\} dx}.$$

Therefore, to compute the marginal density, we have

$$\begin{aligned} p(z | \theta_1, \theta_2, \theta_3) &= \int_{-\infty}^{\infty} h(z) H(\theta_1, \theta_2) \exp\{(T(z) + \theta_1)^T x - (\theta_2 + \theta_3)^T A(x)\} dx \\ &= h(z) \frac{H(\theta_1, \theta_2)}{H(\theta_1 + T(z), \theta_2 + \theta_3)}. \end{aligned}$$

Similarly, the computation of the conditional density is straightforward

$$\begin{aligned} p(x | z, \theta_1, \theta_2, \theta_3) &= \frac{h(z) H(\theta_1, \theta_2) \exp\{(T(z) + \theta_1)^T x - (\theta_2 + \theta_3)^T A(x)\}}{h(z) \frac{H(\theta_1, \theta_2)}{H(\theta_1 + T(z), \theta_2 + \theta_3)}} \\ &= H(\theta_1 + T(z), \theta_2 + \theta_3) \exp\{x^T (\theta_1 + T(z)) - (\theta_2 + \theta_3)^T A(x)\} \\ &= p(x | \theta_1 + T(z), \theta_2 + \theta_3). \end{aligned}$$

This completes the proof. \square

A.2 Proof of Theorem 2

Proof. This follows as a standard application of OLS properties. First, write

$$\begin{aligned} \hat{\beta}(M) &= (X_M^T X_M)^{-1} X_M^T g(Y) = (X_M^T X_M)^{-1} X_M^T [\mu + \epsilon - \frac{1}{\tau} Z] \\ &= \beta^*(M) + (X_M^T X_M)^{-1} X_M^T [\epsilon - \frac{1}{\tau} Z]. \end{aligned}$$

From Section 1, we know that $(\epsilon - \frac{1}{\tau} Z) \sim N(0, (1 + \tau^{-2})\Sigma)$. Therefore

$$\hat{\beta}(M) \sim N(\beta^*(M), (1 + \tau^{-2})(X_M^T X_M)^{-1} X_M^T \Sigma X_M (X_M^T X_M)^{-1}).$$

The coverage statement then follows straightforwardly from the definition of a CI and the properties of the multivariate Gaussian distribution. \square

A.3 Proof of Corollary 1

Proof. It follows directly from Theorem 2 that

$$\hat{\beta}(A) \sim N(\beta^*(A), (1 + \tau^{-2})(A^T A)^{-1} A^T \Sigma A (A^T A)^{-1}).$$

To conclude, simply multiply by $a(x_i)^T$ and apply standard properties of the Gaussian distribution. \square

A.4 Extension to unknown variance in Gaussian linear regression

In the case where p is fixed, $n \rightarrow \infty$, and $\Sigma = \sigma^2 I_n$ we can extend the argument in Section 4 to accommodate unknown variance. In this setting, if we take $\hat{\sigma}^2$ to be the variance estimated from the

residuals by fitting the *full* model with all p covariates, it is a consistent estimate of σ^2 . See section 5.3 of [Tian and Taylor \(2017\)](#) for further details.

We can then modify the definition of $f(Y)$ and $g(Y)$ as follows:

$$f(Y) = Y + \hat{\sigma}\tau Z, \quad \text{and} \quad g(Y) = Y - \frac{\hat{\sigma}}{\tau}Z. \quad (9)$$

where $Z \sim N(0, I_n)$. We can then modify [Theorem 2](#) in a natural way to get an asymptotic coverage guarantee:

Theorem 3. *Let $\hat{\beta}(M)$ be defined as in (3) and $\beta^*(M)$ be defined as in (4). If $f(Y)$ and $g(Y)$ are defined as in (9) and $\Sigma = \sigma^2 I_n$, then the following holds:*

$$\hat{\beta}(M) \xrightarrow{d} N(\beta^*(M), (1 + \tau^{-2})\sigma^2(X_M^T X_M)^{-1}).$$

Furthermore, if $\hat{\sigma}$ is a consistent estimate of σ , we can form an asymptotic $1 - \alpha$ CI for the k th element of $\beta^*(M)$ as

$$\hat{\beta}^k(M) \pm \hat{\sigma}z_{\alpha/2}\sqrt{(1 + \tau^{-2})[(X_M^T X_M)^{-1}]_{kk}}.$$

Proof. By assumption, we know $\hat{\sigma}^2 \xrightarrow{P} \sigma^2$. By Slutsky's theorem, $\frac{Y}{\hat{\sigma}} \xrightarrow{d} N(\frac{\mu}{\sigma}, I_n)$. Draw an independent $Z \sim N(0, I_n)$ and define $f_0(Y) = \frac{Y}{\hat{\sigma}} + \tau Z$ and $g_0(Y) = \frac{Y}{\hat{\sigma}} - \frac{1}{\tau}Z$. Applying the continuous mapping theorem to the joint density of $(\frac{Y}{\hat{\sigma}}, Z)$ implies that

$$(f_0(Y), g_0(Y))^T \xrightarrow{d} N\left(\frac{\mu}{\sigma}, \begin{pmatrix} (1 + \tau^2)I_n & 0 \\ 0 & (1 + \frac{1}{\tau^2})I_n \end{pmatrix}\right).$$

Applying Slutsky's theorem once more and noting that $f(Y) = \hat{\sigma}f_0(Y)$ and $g(Y) = \hat{\sigma}g_0(Y)$ gives us

$$(f(Y), g(Y))^T \xrightarrow{d} N\left(\mu, \begin{pmatrix} \sigma^2(1 + \tau^2)I_n & 0 \\ 0 & \sigma^2(1 + \frac{1}{\tau^2})I_n \end{pmatrix}\right).$$

Applying the continuous mapping theorem once more to the definition of $\hat{\beta}(M)$ and repeating the arguments in [Theorem 2](#) gives us that

$$\hat{\beta}(M) \xrightarrow{d} N(\beta^*(M), (1 + \tau^{-2})\sigma^2(X_M^T X_M)^{-1}).$$

The coverage statement for the CI then follows from standard properties of a Gaussian distribution. \square

A.5 Technical exposition of QMLE procedures

Recall the setting described in [Section 5](#). To recap, after observing $f(Y)$ and X to select a model $M \subseteq [p]$, we conduct inference using a working model of the density for $g(y_i)|f(Y), X$ which we denote $p(g(y_i)|\beta, f(Y), X_M)$. Denote the true mean $\mu_i = \mathbb{E}[g(y_i)|f(Y), X]$ and true variance $\text{Var}[g(y_i)|f(Y), X] = \sigma_i^2$ with $\mu = (\mu_1, \dots, \mu_n)^T$.

The working model implicitly defines a quasi-likelihood function

$$L_n(\beta) := \sum_{i=1}^n \log p(g(y_i)|\beta, f(Y), X_M).$$

We assume that: (i) the support of p does not depend on β , (ii) the quasi-likelihood is twice differentiable with respect to β , and (iii) integration and differentiation with respect to β may be

interchanged. Under these assumptions, we make note of the corresponding quantities of interest: $s_n(\beta) = \frac{\partial L_n}{\partial \beta}$, $H_n(\beta) = -\frac{\partial^2 L_n}{\partial \beta \partial \beta^T}$, and $V_n(\beta) = \text{Var}(s_n(\beta))$.

Under the assumption that $\mathbb{E}(H_n(\beta))$ is positive definite, the target parameter $\beta_n^*(M)$ is defined as the root of $E(s_n(\beta))$. We define $\hat{\beta}_n(M)$ to be an estimator which maximizes the observed score functions $s_n(\beta)$.

Definition 1 (Asymptotic existence). *If $P\left(s_n(\hat{\beta}_n(M)) = 0, H_n(\hat{\beta}_n(M)) \text{ is p.d.}\right) \rightarrow 1$ as $n \rightarrow \infty$, then $\hat{\beta}_n(M)$ asymptotically exists.*

Under the assumption that $\hat{\beta}_n(M)$ asymptotically exists, we study its convergence to $\beta_n^*(M)$. Note that there is no guarantee that $\beta_n^*(M)$ itself converges to a single value — it is a *sequence* that may not converge to anything in general, as it implicitly depends on the sequence of covariates that is observed for each data point. This is a consequence of the fixed-design nature of the regression problem. For random and independent x_i , we can guarantee $\beta^*(M) := \beta_n^*(M)$ will be a single unique value, as described in [White \(1982\)](#).

We make the following assumptions about the sequence of target parameters $\beta_n^*(M)$.

- **(D)** Divergence: $\lambda_{\min}\{V_n(\beta_n^*(M))\} \rightarrow \infty$.
- **(B)** Bounded from above and below: There exist a c , C , and T such that
 1. $\mathbb{P}\left(\lambda_{\min}\{V_n^{-1/2}(\beta_n^*(M))H_n(\beta_n^*(M))V_n^{-T/2}(\beta_n^*(M))\} \geq c > 0\right) \rightarrow 1$,
 2. $\mathbb{P}\left(\lambda_{\max}\{V_n^{-1/2}(\beta_n^*(M))H_n(\beta_n^*(M))V_n^{-T/2}(\beta_n^*(M))\} \leq C < \infty\right) \rightarrow 1$.
- **(S)** Smoothness: For all $\delta > 0$,

$$\max_{\beta: \|V_n^{T/2}(\beta_n^*(M))(\beta - \beta_n^*(M))\| \leq \delta} \left\| H_n^{-1/2}(\beta_n^*(M))H_n(\beta)H_n^{-T/2}(\beta_n^*(M)) - I \right\|_2 \xrightarrow{P} 0.$$

- **(N)** Lindeberg-Feller condition for asymptotic normality holds for any $\epsilon > 0$:

$$\sum_{i=1}^n \mathbb{E}[a_i^T V_n^{-1}(\beta_n^*(M))a_i \mathbb{1}\{a_i^T V_n(\beta_n^*(M))a_i \geq \epsilon^2\}] \rightarrow 0,$$

where $a_i = s_i(\beta_n^*(M)) - s_{i-1}(\beta_n^*(M))$.

Theorem 4 ([Fahrmeir \(1990, Theorem 4\)](#)). *Suppose $p(g(y_i)|\beta, X_M, f(Y))$ is such that (D), (B1) and (S) hold. If $\beta_n^*(M)$ exists, then $\hat{\beta}_n(M)$ exists asymptotically and $\hat{\beta}_n(M) \xrightarrow{P} \beta_n^*(M)$. If (B2) and (N) also hold, then $V_n^{-1/2}(\beta_n^*(M))H_n(\beta_n^*(M))\left(\hat{\beta}_n(M) - \beta_n^*(M)\right) \xrightarrow{d} N(0, I)$.*

In cases of correct specification, $H_n(\beta_n^*(M)) = V_n(\beta_n^*(M))$ which recovers the usual formula for the asymptotic distribution of $\hat{\beta}$.

All that remains is finding plug-in estimators for H_n and V_n . To ease notation, let $\hat{H}_n := H_n(\hat{\beta}_n(M))$ which is consistent due to the continuous mapping theorem. There is no known consistent estimator for $V_n(\beta_n^*(M))$, but we can find an overestimate by using $\hat{V}_n := s_n(\hat{\beta}_n(M))s_n(\hat{\beta}_n(M))^T$. This is motivated by the fact that $\mathbb{E}[s_n(\beta_n^*(M))s_n(\beta_n^*(M))^T] = \text{Var}(s_n(\beta_n^*(M))) + \mathbb{E}[s_n(\beta_n^*(M))]\mathbb{E}[s_n(\beta_n^*(M))]^T$. The last term is positive semidefinite and will generally be small compared to the first term, since the score function should be small if the working model is chosen well. This results in asymptotically *conservative* confidence intervals when used as a plug-in estimator.

Theorem 5. Assume the conditions of [Theorem 4](#) hold. We can then form an asymptotically conservative $1 - \alpha$ CI for the k th element of $\beta_n^*(M)$ as $[\hat{\beta}_n(M)]_k \pm z_{\alpha/2} \sqrt{[\hat{H}_n^{-1} \hat{V}_n \hat{H}_n^{-1}]_{kk}}$.

Proof. [Theorem 4](#) demonstrates that $\hat{\beta}_n(M) \xrightarrow{P} \beta_n^*(M)$. Due to the assumption that the quasi-likelihood function is twice continuously differentiable, H_n and s_n are both continuous functions with respect to β , so by the continuous mapping theorem, $\hat{H}_n \xrightarrow{P} H_n(\beta_n^*(M))$ and $s_n(\hat{\beta}_n(M)) \xrightarrow{P} s_n(\beta_n^*(M))$. In the rest of the argument, we drop the explicit dependence on the selected model (M) to avoid clunky notation and therefore let $\hat{\beta}_n := \hat{\beta}_n(M)$ and $\beta_n^* := \beta_n^*(M)$ in the arguments that follow. Now, note that

$$\mathbb{E}[s_n(\beta_n^*)s_n(\beta_n^*)^T] = \text{Var}(s_n(\beta_n^*)) + \mathbb{E}[s_n(\beta_n^*)]\mathbb{E}[s_n(\beta_n^*)]^T$$

where the last term is positive semidefinite since it is a Gram matrix. Recall that if two matrices A, B are positive semidefinite then ABA is positive semidefinite and A^{-1} is positive semidefinite when A is invertible. Since $H_n(\beta_n^*)$ is also positive semidefinite by assumption, we know that

$$H_n^{-1}(\beta_n^*) \left(\mathbb{E}[s_n(\beta_n^*)s_n(\beta_n^*)^T] - V_n(\beta_n^*) \right) H_n^{-1}(\beta_n^*)$$

is positive semidefinite.

Denote the Cholesky decomposition of $H_n^{-1}(\beta_n^*) \mathbb{E}[s_n(\beta_n^*)s_n(\beta_n^*)^T] H_n^{-1}(\beta_n^*)$ as LL^T and the Cholesky decomposition of $H_n^{-1}(\beta_n^*) V_n(\beta_n^*) H_n^{-1}(\beta_n^*)$ as MM^T . From the above, we know that $LL^T - MM^T$ is positive semidefinite which implies that

$$L_{kk} - M_{kk} = \sqrt{[H_n^{-1}(\beta_n^*) \mathbb{E}[s_n(\beta_n^*)s_n(\beta_n^*)^T] H_n^{-1}(\beta_n^*)]_{kk}} - \sqrt{[H_n^{-1}(\beta_n^*) V_n(\beta_n^*) H_n^{-1}(\beta_n^*)]_{kk}}$$

must be greater than 0 since the diagonal entries must be positive.

By the WLLN, $\hat{V}_n \xrightarrow{P} \mathbb{E}[s_n(\beta_n^*)s_n(\beta_n^*)^T]$ which combined with the above statement shows us

$$\lim_{n \rightarrow \infty} P \left(\sqrt{[\hat{H}_n^{-1} \hat{V}_n \hat{H}_n^{-1}]_{kk}} \geq \sqrt{[H_n^{-1}(\beta_n^*) V_n(\beta_n^*) H_n^{-1}(\beta_n^*)]_{kk}} \right) = 1. \quad (10)$$

Putting everything together, we have that

$$\begin{aligned} 1 - \alpha &= \lim_{n \rightarrow \infty} P \left([\beta_n^*]_k \in \left[[\hat{\beta}_n]_k \pm z_{\alpha/2} M_{kk} \right] \right) \\ &\leq \lim_{n \rightarrow \infty} P \left([\beta_n^*]_k \in \left[[\hat{\beta}_n]_k \pm z_{\alpha/2} \sqrt{[\hat{H}_n^{-1} \hat{V}_n \hat{H}_n^{-1}]_{kk}} \right] \right), \end{aligned}$$

where the first line follows from [Theorem 4](#) and the second line follows from (10). □

We now demonstrate how to apply [Theorem 5](#) in the context of generalized linear models which we then use for the simulations discussed in [Section 5](#) and Appendices [E.3](#) and [E.4](#). We restrict attention to working models in the *exponential dispersion* family, i.e., with a density $p(g(y_i)|f(Y), X) = \exp\left(\frac{y_i \theta_i - b(\theta_i)}{a(\phi)} + c(g(y_i), \phi)\right)$ for some functions $a(\cdot), b(\cdot), c(\cdot, \cdot)$. Denote $m = (m_1, \dots, m_n)^T$ to be the mean under the assumption of the working model and $v = (v_1, \dots, v_n)^T$ to be the variance under the assumption of the working model. The covariates are linked to the (assumed) random component through a *link function* h where $\eta_i := \beta^T \tilde{x}_i$ and $\eta_i = h(m_i)$. The equations defined in the preceding

section simplify to

$$\begin{aligned} s_n(\beta) &= X_M^T D V^{-1} (g(Y) - m), \\ H_n(\beta_n^*(M)) &= \sum_{i=1}^n \tilde{x}_i \left(\frac{\partial m_i}{\partial \eta_i} \right)^2 v_i^{-1} \tilde{x}_i^T = X_M^T D^2 V^{-1} X_M, \\ V_n(\beta_n^*(M)) &= \sum_{i=1}^n \tilde{x}_i \left(\frac{\partial m_i}{\partial \eta_i} \right)^2 \frac{\sigma_i^2}{v_i^2} \tilde{x}_i^T = X_M^T D^2 \Sigma V^{-2} X_M, \end{aligned}$$

where D, V, Σ are diagonal matrices with $D_{ii} = \frac{\partial m_i}{\partial \eta_i}$, $V_{ii} = v_i$, and $\Sigma_{ii} = \sigma_i^2$. Furthermore, we can rewrite the plug-in estimator described above as

$$\hat{V}_n := s_n(\hat{\beta}_n(M)) s_n(\hat{\beta}_n(M))^T = \sum_{i=1}^n \tilde{x}_i (g(y_i) - m_i)^2 v_i^{-2} \left(\frac{\partial m_i}{\partial \eta_i} \right)^2 \tilde{x}_i^T.$$

We now apply these equations to three prototypical examples of GLMs (Gaussian regression, Poisson regression, logistic regression).

Example 1: Gaussian linear regression Assume that we have split Y into two pieces $f(Y)$ and $g(Y)$ using one of the methodologies in [Section 2.2](#) but the post-selective likelihood function cannot be conveniently modeled. As a simplifying assumption, an analyst decides to model $g(Y)$ using linear regression with a selected model $M \subseteq [p]$ and an assumption of Gaussian errors but wants to conduct inference in a way that is robust to misspecification. If the analyst models the data as homoscedastic with common variance σ_0^2 , then the score equation simplifies as $s_n(\beta) = X_M^T (g(Y) - X_M \beta)$, leading to the standard estimator of $\hat{\beta}_n(M) = (X_M^T X_M)^{-1} X_M^T g(Y)$. We have our plug-in variance estimator:

$$\begin{aligned} \hat{H}_n^{-1} \hat{V}_n \hat{H}_n^{-1} &= (\sigma_0^2 X_M^T X_M)^{-1} \left(X_M^T \text{diag} \left(\frac{g(Y) - X_M \hat{\beta}}{\sigma_0^4} \right) X_M \right) (\sigma_0^2 X_M^T X_M)^{-1} \\ &= (X_M^T X_M)^{-1} X_M^T \text{diag} \left(g(Y) - X_M \hat{\beta} \right) X_M (X_M^T X_M)^{-1}, \end{aligned}$$

which is exactly the sandwich estimator of [White \(1980\)](#). However, in this context, the estimator is an overestimate for $\beta_n^*(M)$ and leads to conservative rather than exact CIs.

Example 2: Poisson regression Considering $y_i \sim \text{Pois}(\mu)$, we fission the data as in [Section 2.2](#) with $f(Y_i) \sim \text{Bin}(Y_i, p)$ with $g(y_i) = y_i - f(y_i)$. We then attempt to model $g(y_i)$ using a GLM with log link function using selected covariates $x_{i \cdot M}$ and an offset of $\log(1-p)$ to account for the randomization.

We assume that the true distribution of the data is indeed Poisson but the mean $\mathbb{E}(y_i | x_i)$ may not be a linear function of the chosen covariates \tilde{x}_i . The constructed CIs will then cover the target parameters $\beta_n^*(M)$ that minimizes the KL divergence between the true and the modeled distribution:

$$\beta_n^*(M) := \underset{\beta}{\text{argmin}} D_{KL} \left(\prod_{i=1}^n q((1-p)\mu_i) \parallel \prod_{i=1}^n q(\exp\{\log(1-p) + \beta^T \tilde{x}_i\}) \right),$$

where $q(\cdot)$ is the distribution of Poisson distribution as a function of its mean.

For this problem, we have that $\frac{\partial m_i}{\partial \eta_i} = m_i = v_i = \exp(\beta^T \tilde{x}_i)$. This leads to the plug-in estimator for variance to be

$$\hat{H}_n^{-1} \hat{V}_n \hat{H}_n^{-1} = \left(X_M^T \hat{V} X_M \right)^{-1} \left(X_M^T \hat{D} X_M \right) \left(X_M^T \hat{V} X_M \right)^{-1}, \quad (11)$$

where \hat{D} and \hat{V} are diagonal matrices with $\hat{D}_{ii} = g(y_i) - (1-p) \exp(\hat{\beta}^T \tilde{x}_i)$ and $\hat{V}_{ii} = (1-p) \exp(\hat{\beta}^T \tilde{x}_i)$.

Example 3: Logistic regression Assume that $y_i \sim \text{Ber}(\mu_i)$ and we fission the data into $f(y_i) \sim \text{Ber}(\mu_i + p - 2p\mu_i)$ and $g(y_i)|f(y_i) \sim \text{Ber}\left(\frac{\mu_i}{\mu_i + (1-\mu_i)[p/(1-p)]^{2f(y_i)-1}}\right)$ as described in [Section 2.2](#). Modelling this likelihood is challenging because the function is non-convex, so it may be easier to try and use a logistic regression with selected covariates \tilde{x}_i to model this probability even though the post-selective distribution does not have this functional form. As before, we can still interpret the fitted parameters from a logistic regression as the projection onto the working model. For this problem, we have that $\frac{\partial m_i}{\partial \eta_i} = m_i(1 - m_i) = v_i$. This leads to the plug-in estimator for variance to be the same as in (11) except with $\hat{D}_{ii} = g(y_i) - \hat{m}_i$ and $\hat{V}_{ii} = \hat{m}_i(1 - \hat{m}_i)$ with $\hat{m}_i = \frac{1}{1 + \exp(-\hat{\beta}^T \tilde{x}_i)}$.

B List of decompositions

Included in this section is a more extensive list of distributions for several commonly encountered distributions. When discussing each method, we will label them as follows so the reader will be able to relate them easily to the strategies discussed in [Section 2](#):

- **(P1)** will indicate that the decomposition strategy is an instance of the first principle — $f(X)$ and $g(X)$ are independent with known distributions.
- **(P2)** will indicate that the decomposition strategy follows the second principle — $f(X)$ has a known marginal distribution, while $g(X)$ has a known conditional distribution given $f(X)$.
- **(P2 CP)** will indicate that the decomposition strategy is an instance of the second principle — but specifically using “conjugate-prior reversal”.

Although we recognize readers may find a close reading of this section tedious, we feel it is important to include this information for two reasons. First, we wish to provide several concrete examples to demonstrate to the reader how the strategies for constructing $f(X)$ and $g(X)$ can be practically instantiated in settings beyond the specific applications found in this paper. Second, we want to highlight the wide applicability of this approach to disparate problems within statistics — only providing a small number of examples would give the false impression that this methodology is only tractable within a few idealized settings.

- **Gaussian**

1. **(P1)** Suppose $X \sim N(\mu, \Sigma)$ is d -dimensional ($d \geq 1$). Draw $Z \sim N(0, \Sigma)$. Then $f(X) = X + \tau Z$, where $\tau \in (0, \infty)$ is a tuning parameter, has distribution $N(\mu, (1 + \tau^2)\Sigma)$; and $g(X) = X - \frac{1}{\tau}Z$ has distribution $N(\mu, (1 + \tau^{-2})\Sigma)$; and $f(X) \perp\!\!\!\perp g(X)$. Larger τ indicates less informative $f(X)$ (and more informative $g(X) | f(X)$).
2. **(P2 CP)** Alternatively, draw $Z \sim N(X, \tau\Sigma)$, where $\tau \in (0, \infty)$ is a tuning parameter. Then $f(X) = Z$ has marginal distribution $N(\mu, (1 + \tau)\Sigma)$; and $g(X) = X$ has conditional distribution $N(\frac{\tau}{\tau+1}(\mu + f(X))/\tau, \frac{\tau}{\tau+1}\Sigma)$. Larger τ indicates less informative $f(X)$.
3. **(P2)** More generally, we can add Gaussian noise with an arbitrary covariance matrix. Draw $Z \sim N(0, \Sigma_0)$ and let $f(X) = X - Z$ with $g(X) = X + Z$ as before. For notational convenience, let $\Sigma_1 = \Sigma + \Sigma_0$ and $\Sigma_2 = \Sigma - \Sigma_0$. Then $f(X) \sim N(\mu, \Sigma + \Sigma_0)$ and $g(X)|f(X) \sim N(\mu + \Sigma_2 \Sigma_1^{-1} (f(X) - \mu), \Sigma_1 - \Sigma_2 \Sigma_1^{-1} \Sigma_2)$.

- **Gamma**

1. **Exponential (P2 CP)** Suppose $X \sim \text{Exp}(\theta)$. Draw $Z = (Z_1, \dots, Z_B)$ where each element is i.i.d. $Z_i \sim \text{Poi}(X)$ and $B \in \{1, 2, \dots\}$ is a tuning parameter. Then $f(X) = Z$, where each element is independently distributed as $\text{Geo}(\frac{\theta}{\theta+B})$. $g(X) = X$ has conditional distribution $\text{Gamma}(1 + \sum_{i=1}^B f_i(X), \theta + B)$. Larger B indicates more informative $f(X)$ (and less informative $g(X) | f(X)$).
(P2 CP) Alternatively, we can draw $Z \sim \text{Poi}(\tau X)$, where $\tau \in (0, \infty)$ is a tuning parameter. Then $f(X) = Z$, marginally distributed as $\text{Geo}(\frac{\theta}{\theta+\tau})$. $g(X) = X$ has conditional distribution $\text{Gamma}(1 + f(X), \theta + \tau)$. Here, $f(X)$ is most informative when τ is comparable with θ , and less informative when τ approaches 0 or ∞ .
2. **(P2 CP)** Generally, suppose $X \sim \text{Gamma}(\alpha, \beta)$. Draw $Z = (Z_1, \dots, Z_B)$ where each element is i.i.d. $Z_i \sim \text{Poi}(X)$ and $B \in \{1, 2, \dots\}$ is a tuning parameter. Then $f(X) = Z$, where each element is independently distributed as a negative binomial $NB(\alpha, \frac{1}{\beta+1})$. $g(X) = X$ has conditional distribution $\text{Gamma}(\alpha + \sum_{i=1}^B f_i(X), \beta + B)$. Larger B indicates more informative $f(X)$ (and less informative $g(X) | f(X)$).
3. **(P2 CP)** Alternatively, we can draw $Z \sim \text{Poi}(\tau X)$, where $\tau \in (0, \infty)$ is a tuning parameter. Then $f(X) = Z$, marginally distributed as $NB(\alpha, \frac{\tau}{\beta+\tau})$. $g(X) = X$ has conditional distribution $\text{Gamma}(\alpha + f(X), \beta + \tau)$. $f(X)$ is most informative when τ is comparable with θ , and less informative when τ approaches zero or infinity.
4. Note: decomposition of the Gamma distribution implies decomposition of the Chi-square distribution χ_k^2 , as it is equivalent to $\text{Gamma}(k/2, 1/2)$.

- **Beta**

1. **(P2 CP)** Suppose $X \sim \text{Beta}(\theta, 1)$. Draw $Z \sim \text{Bin}(B, X)$, where $B \in \{1, 2, \dots\}$ is a tuning parameter. Then $f(X) = Z$ has marginal distribution as a discrete uniform in $\{0, 1, \dots, B\}$ when $\theta = 1$, and stochastically larger (smaller) than a discrete uniform when θ is larger (smaller) than one (the PMF of Z is $p_\theta(z) = \frac{\theta \Gamma(z+\theta) B!}{\Gamma(B+1+\theta) z!}$). $g(X) = X$ has conditional distribution $\text{Beta}(\theta + f(X), B - f(X) + 1)$. Larger B indicates more informative $f(X)$ (and less informative $g(X) | f(X)$).
2. **(P2 CP)** Similarly, if $X \sim \text{Beta}(1, \theta)$, we can draw $Z \sim \text{Bin}(B, 1 - X)$, and the resulting $f(X), g(X)$ have the same (conditional) distributions as above.
3. **Multivariate case: Dirichlet (P2 CP)** Suppose $X \sim \text{Dir}(\theta, 1, \dots, 1)$, where $(\theta, 1, \dots, 1)$ is a d -dimensional vector with $k \geq 2$. Draw $Z \sim \text{Multinom}(B, X)$, where $B \in \{1, 2, \dots\}$ is a tuning parameter. Then $f(X) = Z$ has marginal distribution as a discrete uniform in its support $\{z_i \in \{0, \dots, B\} \text{ for } i \in [d] : \sum_{i=1}^d z_i = B\}$ when $\theta = 1$, and for other θ , the PMF is $p_\theta(z) = \frac{B! \Gamma(\theta) \Gamma(B+d-1+\theta)}{z_1! \Gamma(\theta) \Gamma(B+d-1+\theta)}$. $g(X) = X$ has conditional distribution $\text{Dir}(\theta + f_1(X), 1 + f_2(X), \dots, 1 + f_k(X))$. Larger B indicates more informative $f(X)$ (and less informative $g(X) | f(X)$).

In the general case, where $X \sim \text{Dir}(\theta_1, \theta_2, \dots, \theta_d)$, we can use the same construction. Then $f(X) = Z$ has marginal distribution

$$p_\theta(z) = \frac{\Gamma\left(\sum_{i=1}^d \theta_i\right) \left[\prod_{i=1}^d \Gamma(z_i + \theta)\right] n!}{\Gamma\left(n + \sum_{i=1}^d \theta_i\right) \left[\prod_{i=1}^d \Gamma(\theta_i)\right] \left[\prod_{i=1}^d z_i!\right]}.$$

$g(X) = X$ has conditional distribution $\text{Dir}(\theta_1 + f_1(X), \dots, \theta_k + f_d(X))$. Larger B indicates more informative $f(X)$ (and less informative $g(X) | f(X)$).

- **Binomial (P2).** Suppose $X \sim \text{Bin}(n, \theta)$. Draw $Z \sim \text{Bin}(X, p)$ where $p \in (0, 1)$ is a tuning parameter. Then $f(X) = Z$ has marginal distribution $\text{Bin}(n, p\theta)$; and $g(X) = X - Z$ has

conditional distribution as $\text{Bin}(n - Z, \frac{1-\theta}{1-p\theta})$. Larger p indicates more informative $f(X)$. Note that the decomposition of Binomial is not trivially applicable to Bernoulli distribution since $X = 1$ with probability one if $Z = 1$.

- **Bernoulli (P2)**. Suppose $X \sim \text{Ber}(\theta)$. Draw $Z \sim \text{Ber}(p)$ where $p \in (0, 1)$ is a tuning parameter. Then $f(X) = X(1 - Z) + (1 - X)Z$ has marginal distribution $\text{Ber}(\theta + p - 2p\theta)$; and $g(X) = X$ has conditional distribution (given $f(X)$) as $\text{Ber}\left(\frac{\theta}{\theta + (1-\theta)[p/(1-p)]^{2f(X)-1}}\right)$. Smaller p indicates more information in $f(X)$.
- **Categorical (P2)**. Suppose $X \sim \text{Cat}(\theta_1, \dots, \theta_d)$. Draw $Z \sim \text{Ber}(p)$ where $p \in (0, 1)$ is a tuning parameter. Also draw $D \sim \text{Cat}(\frac{1}{d}, \dots, \frac{1}{d})$. Let $f(X) = X(1 - Z) + DZ$ and $g(X) = X$. Then $f(X) \sim \text{Cat}(\phi_1, \dots, \phi_d)$ with $\phi_i = (1 - p)\theta_i + \frac{p}{d}$. Furthermore $g(X)|f(X)$ has distribution

$$p_\theta(g(X) = s | f(X) = t) = \begin{cases} \frac{(1-p+\frac{p}{d})\theta_s}{(1-p)\theta_s+p/d} & \text{if } s = t \\ \frac{\theta_t \frac{p}{d}}{(1-p)\theta_t+p/d} & \text{if } s \neq t. \end{cases}$$

Larger p indicates more informative $f(X)$. Note that there is nothing special about choosing $\frac{1}{d}$ above, the method generalizes to any vector of probabilities for D . When $d = 2$, substituting $1 - X$ for D in the above construction recovers the Bernoulli decomposition given above.

- **Poisson**

1. **(P1)** Suppose $X \sim \text{Poi}(\mu)$. Draw $Z \sim \text{Bin}(X, p)$ where $p \in (0, 1)$ is a tuning parameter. Then $f(X) = Z$ has marginal distribution $\text{Poi}(p\mu)$; and $g(X) = X - Z$ is independent of $f(X)$ and distributes as $\text{Poi}((1 - p)\mu)$. Larger p indicates more informative $f(X)$.
 2. **(P2)** Alternatively, draw $Z \sim \text{Poi}(p)$. We can then exploit the thinning property of the Poisson distribution ([Last and Penrose \(2017\)](#)) to construct $f(X) = X + Z \sim \text{Poi}(\mu + p)$. Letting $X = g(X)$ gives $g(X)|f(X) \sim \text{Bin}\left(f(X), \frac{\mu}{\mu+p}\right)$. Larger p corresponds to a less informative $f(X)$ (and more informative $g(X)|f(X)$).
- **Negative Binomial (P2)**. Suppose $X \sim \text{NB}(r, \theta)$. Draw $Z \sim \text{Bin}(X, p)$ where $p \in (0, 1)$ is a tuning parameter. Then $f(X) = Z$ has marginal distribution $\text{NB}(r, \frac{\theta}{\theta+p-p\theta})$; and $g(X) = X - Z$ has conditional distribution $\text{NB}(r + Z, \theta + p - p\theta)$. Larger p indicates more informative $f(X)$. A special case of Negative Binomial is geometric distribution where $r = 1$.

Remark 3 (Relationship to infinite divisibility.). *Note that we are able to decompose Poisson, Binomial, and Negative Binomial by drawing a Binomial distribution with size X , which is a generic formulation. Poisson and Negative Binomial belong to the class of discrete compound Poisson distribution (DCP) with parameters $(\lambda\alpha_1, \lambda\alpha_2, \dots)$, where:*

$$\mathbb{E}(t^X) \equiv \sum_{x=0}^{\infty} \mathbb{P}(X = x)t^x = \exp\left\{\sum_{k=1}^{\infty} \alpha_k \lambda(t^k - 1)\right\}, \quad (12)$$

for $|t| \leq 1$. It is equivalent to saying that X is infinitely divisible. We note that if X follows a DCP with parameter $(\lambda\alpha_1, \lambda\alpha_2, \dots)$ and we draw $Z \sim \text{Bin}(X, p)$, then Z marginally follows a DCP with parameter $(\sum_{k=1}^{\infty} \alpha_k \lambda k(1-p)^{k-1}p, \dots, \sum_{k=i}^{\infty} \alpha_k \lambda \binom{k}{i}(1-p)^{k-i}p^i, \dots)$. However, it may not be true in general that $X | Z$ also follows a (shifted) DCP when X is DCP. These examples are simply three cases where the conditional distribution is tractable.

C Comparison between data splitting and data fission in fixed-design linear regression

We can give an analogous statement about how this data fission procedure relates to data splitting for fixed-design linear regression as the one made in [Example 1](#). For data splitting, we pick $a \in \{\frac{1}{n}, \dots, \frac{n-1}{n}, 1\}$ and set aside the first an observations for selection and the remaining $(1-a)n$ observations for inference. We then select some model $M \subseteq [p]$ during the selection stage. This restricts us to a smaller model design matrix $X_M^{\text{inf}} \in \mathbb{R}^{(1-a)n \times |M|}$ for inference. Also denote Σ_{inf} the covariance matrix for the error term of these $(1-a)n$ observations. Then,

$$\widehat{\beta}_{\text{split}} \sim N(\beta^*(M), (X_M^{\text{inf}T} X_M^{\text{inf}})^{-1} X_M^{\text{inf}T} \Sigma_{\text{inf}} X_M^{\text{inf}} (X_M^{\text{inf}T} X_M^{\text{inf}})^{-1}).$$

For data fission, let us denote the model chosen during the selection stage as $M^\circ \subseteq [p]$ and the corresponding model design matrix $X_{M^\circ} \in \mathbb{R}^{n \times |M^\circ|}$. Then,

$$\widehat{\beta}_{\text{fission}} \sim N(\beta^*(M^\circ), (1 + \tau^{-2})(X_{M^\circ}^T X_{M^\circ})^{-1} X_{M^\circ}^T \Sigma X_{M^\circ} (X_{M^\circ}^T X_{M^\circ})^{-1}).$$

Both quantities are unbiased, but determining whether $\widehat{\beta}_{\text{fission}}$ or $\widehat{\beta}_{\text{split}}$ has lower variance depends on too many unknown quantities to say definitively without additional assumptions. First, there is no guarantee that M° and M will be the same — i.e. different models may be selected during the first stage for each of these two procedures. Second, nothing is assumed about the design matrix X so it is hard to say much about how $(X^T X)^{-1}$ changes if restricted to only a subset of rows/columns. However, heuristically, the estimator increases variance when compared with data splitting via randomization through the $1 + \tau^{-2}$ term but decreases variance by increasing the number of rows within the model design matrix. We use an idealized example below to draw more parallels.

Example 2. Assume that we have orthogonal covariates ($X_i^T X_j = 0$ for all $i \neq j$) and known homoscedastic noise (for all i , $\sigma_i^2 = \sigma^2$, for some known σ^2). Also assume that both procedures select the same model $M = M^\circ$. Then $\widehat{\beta}_{\text{fission}} \sim N(\beta^*(M), (1 + \tau^{-2})\sigma^2(X_M^T X_M)^{-1})$ and $\widehat{\beta}_{\text{split}} \sim N(\beta^*(M), \sigma^2(X_M^{\text{inf}T} X_M^{\text{inf}})^{-1})$. Moreover the matrices are easily invertible since $X^T X$ is a diagonal matrix. Therefore, we have:

$$\text{Var}(\beta_j^{\text{fission}}) = \frac{(1 + \tau^{-2})\sigma^2}{\sum_{i=1}^n X_{ij}^2}, \quad \text{and} \quad \text{Var}(\beta_j^{\text{split}}) = \frac{\sigma^2}{\sum_{i=an+1}^n X_{ij}^2}.$$

For a fixed a , the parameter τ that equates these two variances is $\tau = \left(\frac{\sum_{i=1}^{an} X_{ij}^2}{\sum_{i=an+1}^n X_{ij}^2} \right)^{1/2}$.

Although idealized, this example draws attention to a key weakness that data splitting has in fixed-design linear regression. Data fission is always able to smoothly tradeoff the information between the selection and inference datasets through the parameter τ but data splitting is limited in the ways that information can be divided since it requires that the analyst allocate points discretely.

D Background on trend filtering

We include a summary of trend filtering when the order $k > 1$. As before, we consider the problem of estimating the underlying smooth trend of a time series $y_t \in \mathbb{R}$ with $t = 1, \dots, n$ with structural equation.

$$y_t = f_0(t) + \epsilon_t. \tag{13}$$

Our goal is to estimate the underlying trend $(f_0(1), \dots, f_0(n))$. The approach of trend filtering is to fit a piecewise polynomial of degree k to the data with adaptively chosen breakpoints or *knots*. Formally,

the k -th order trend filtering estimator is defined to be $\hat{x} = (\hat{x}_1, \dots, \hat{x}_n)$, which is the solution to the minimization problem

$$\hat{x} = \operatorname{argmin}_{x \in \mathbb{R}^n} \frac{1}{2} \|Y - x\|_2^2 + \lambda \|D^{(k+1)}x\|_1, \quad (14)$$

where $\lambda \geq 0$ is a tuning parameter and k is the order of the piecewise polynomial that is being chosen to fit the data. $D^{(k+1)} \in \mathbb{R}^{(n-k) \times n}$ is the k -th order difference matrix defined recursively by defining

$$D^{(1)} = \begin{bmatrix} -1 & 1 & 0 & \dots & 0 & 0 \\ 0 & -1 & 1 & \dots & 0 & 0 \\ \vdots & & & & & \\ 0 & 0 & 0 & \dots & -1 & 1 \end{bmatrix} \in \mathbb{R}^{(n-k-1)},$$

and $D^{(k+1)} \in \mathbb{R}^{(n-k) \times n}$ as

$$D^{(k+1)} = D^{(1)}D^{(k)}.$$

From this definition, we can see that setting $k = 0$ yields $D^{(k+1)} = D^{(1)}$ which corresponds to fitting a piecewise constant function. This is also known as the 1-dimensional fused lasso problem of Tibshirani et al. (2005). Choosing $k = 1$ corresponds to fitting a piecewise linear function across t , choosing $k = 2$ corresponds to fitting a piecewise quadratic function across t and so on.

Although trend filtering is a relatively recently developed tool in nonparametric statistics, it has gained substantial popularity over the last several years due to it converging to the true underlying function at the minimax rate (see Tibshirani (2014)) in addition to being computationally efficient. The specialized alternation direction method of multipliers (ADMM) algorithm of Ramdas and Tibshirani (2014) converges at the $\mathcal{O}(n^{1.5})$ rate in the worst case but in practice tends to scale extremely well for large datasets. Most other nonparametric estimators that can be computed efficiently such as smoothing splines and uniform-knot regression splines are not locally adaptive and therefore do not converge at the minimax rate. Other methods that are locally adaptive such as the locally adaptive regression spline of Mammen and van de Geer (1997) can be shown to converge at the minimax rate but are not computationally tractable. For a more complete overview of these competing methods and the various ways in which they may tradeoff between their theoretical properties, the interested reader may wish to consult Politsch et al. (2020a).

E Supplemental simulation results

E.1 Simulation results for interactive hypothesis testing

In this section, we provide a more detailed description of the simulation setup in Section 3, additional commentary on the simulation results, and additional demonstrations for non-Gaussian datasets.

Simulation setup The covariates $x_i \in \mathbb{R}^2$ are arranged on a 50×50 grid in the area $[-100, 100] \times [-100, 100]$. We let the set of non-nulls be arranged in a circle in the center of the grid as shown in Figure 4 and set $\mu_i = 2$ for each non-null and $\mu_i = 0$ for each true null. The data is generated as $y_i \sim N(\mu_i, 1)$. We form a rejection set using the BH, AdaPT, and STAR procedures, both with and without data fission. For the non-fissioned versions of these procedures using the full dataset, the (one-sided) p-values that are used are calculated as $p_i^{\text{full}} = 1 - \Phi(y_i)$. Similarly, for the fissioned versions of these procedures, the (one-sided) p-values are calculated as $p_i^{\text{fission}} = 1 - \Phi(f(y_i)(1 + \tau^2)^{-\frac{1}{2}})$. The AdaPT and STAR procedures are designed so that the analyst may explicitly use the covariate information x_i in forming their rejection set, with STAR explicitly imposing a structural constraint that the rejection region needs to be spatially convex (with respect to its covariates x_i). Note that although AdaPT and STAR control the false discovery rate regardless of how the analyst chooses

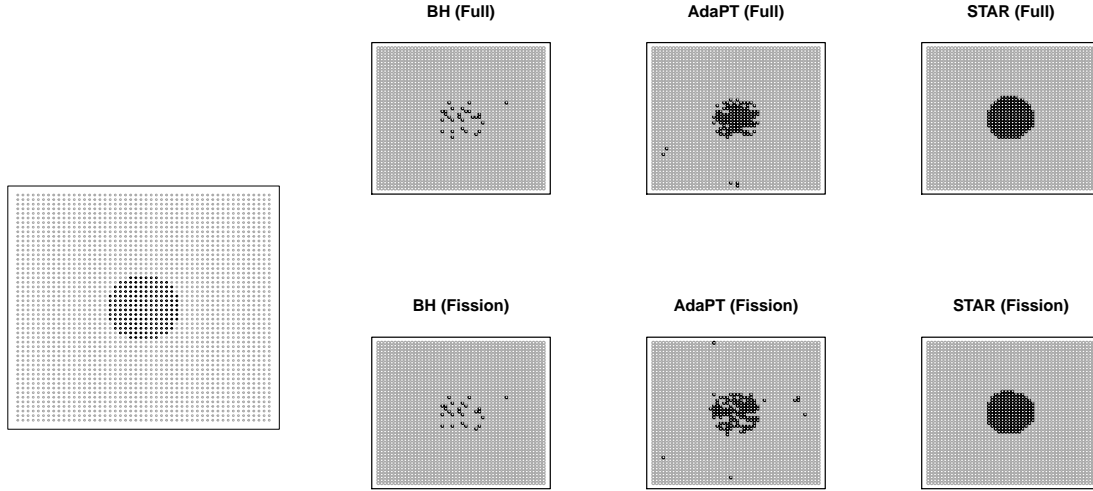


Figure 12. Example rejection region for a single trial run. STAR, AdaPT, and BH procedures are used to try and recover the true signal pattern (left) with a target FDR of 0.1. Fissioning the data (with $\tau = 0.1$) to allow for the estimation of signal strength only mildly impairs the ability of these procedures to correctly identify the rejection region.

to reject their hypotheses with this information, for the purposes of this simulation, we rely on the algorithmic procedures described in Section 4.2 of [Lei et al. \(2020\)](#) and Section 4 of [Lei and Fithian \(2018\)](#) to form the rejection set. Since the BH procedure is not designed to use side information to form a rejection set, its power is significantly lower than the AdaPT and STAR procedures for this simulation.

An example of a rejection set for each of the six methodologies for a single trial run can be seen in [Figure 4](#). We note that the increased variance introduced through fission will necessarily decrease the power of these procedures in the selection phase, but the level of degradation is minor for small values of τ . After forming the rejection sets for the fissioned versions of the datasets, we form CIs to cover $\bar{\mu}$ using the above outlined procedure. As a point of comparison, we also compare this methodology to the invalid procedure of “double dipping” to form CIs on the non-fissioned dataset.

We repeat this simulation over 250 trials for a variety of different τ to observe how information trades off between the selection and inference steps. To measure the effectiveness of our procedure, we track the following metrics for the *selection* stage:

$$\text{Power} := \frac{|x_i \in \mathcal{R} : \mu_i \neq 0|}{|\{i : \mu_i \neq 0\}|}, \quad \text{and} \quad \text{false discovery proportion (FDP)} := \frac{|x_i \in \mathcal{R} : \mu_i = 0|}{\max\{|\mathcal{R}|, 1\}}.$$

For the *inference* stage, we denote the CI created through the data fission procedures that covers $\bar{\mu}$ as $\overline{\text{CI}}$ with lower and upper bounds $\overline{\text{CI}}(1), \overline{\text{CI}}(2)$ and compute the following metrics:

$$\text{Miscoverage} = \mathbb{1}(\bar{\mu} \notin \overline{\text{CI}}), \quad \text{and} \quad \text{CI Length} = |\overline{\text{CI}}(2) - \overline{\text{CI}}(1)|.$$

The results are shown in [Figure 4](#) with target coverage level $1 - \alpha = 0.8$ and target FDR control at 0.2. As τ increases, we see a tradeoff between the power in the selection stage and the CI length in the inference stage. Despite having this general trend, the decrease in CI length is not strictly monotonic with τ in all cases (e.g. the fissioned BH procedure has CI lengths which actually increase from $\tau \approx 0.5$

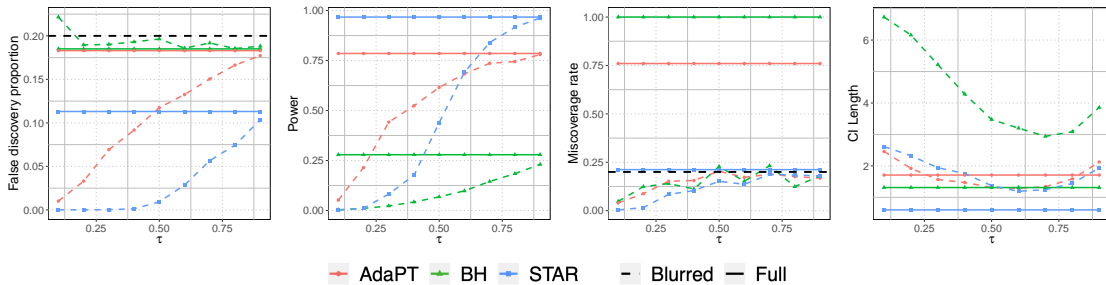


Figure 13. Numerical results for the *selection stage* for a Poisson signal, averaged over 250 trials for a 50×50 grid of hypotheses with target FDR level chosen at 0.2 and τ varying over $\{0.1, 0.2, 0.3, 0.5, 0.6, 0.7, 0.8, 0.9\}$. Solid lines denote metrics for the rejection sets formed using the full dataset and dotted lines denote metrics calculated using the rejection sets formed through data fission. All fission methods control the false discovery rate at the desired coverage level but we can see that increasing τ increases the power of the fissioned procedures as more of the information gets reserved for selection.

to $\tau \approx 1$) because the length of the CIs increases with τ but decreases with $|\mathcal{R}|$. Since the size of the rejection set increases as power increases, moving τ causes these two effects to work in opposite directions. Nonetheless, increasing τ tends to decrease CI length in most instances.

Poisson Data Note that in the preceding examples, Gaussian distributed data were used but this procedure can be modified straightforwardly for data that is distributed in any way such that a decomposition rule (e.g. from [Appendix B](#)) can be applied. Consider a situation where we now observe $y_i \sim \text{Pois}(\mu_i)$ and during the selection stage, we are attempting to form a rejection set against the null hypothesis $H_0 : \mu_i = 1$ compared to the alternative $H_1 : \mu_i > 1$.

One technical note is that in this case, if we calculate the (one-sided) p-value using the straightforward calculation of $p_i = P(Y \leq y_i) : Y \sim \text{Pois}(1)$, the technique of p-value masking will fail to guarantee error control because p_i can be reconstructed from $\min(p_i, 1 - p_i)$ when the distribution is discrete. To account for this, we add an additional layer of randomization when calculating the p-value using [Brockwell \(2007\)](#). Specifically, we draw $U \sim \text{Unif}(0, 1)$ and calculate

$$Y' = F(Y)U + (1 - U)F(Y-),$$

where $F(Y)$ denotes the CDF of a $\text{Pois}(1)$ variable and $F(Y-)$ denotes the corresponding left limit. This ensures that Y' is uniformly distributed and stochastically dominated by $F(Y)$ and is therefore a valid p-value.

To form CIs at the inference stage, we can manually invert the test statistics but a simpler method described in [Ulm \(1990\)](#) provides a convenient shortcut. In particular, the $1 - \alpha$ CI around $\bar{\mu}$ for the CIs constructed from the fissioned data can be calculated as

$$\frac{1}{2|\mathcal{R}|(1 - \tau)} \left(\chi_{\alpha/2}^2 \left(2 \sum_i y_i \right), \chi_{1-\alpha/2}^2 \left(2 \sum_i y_i + 2 \right) \right).$$

Empirical results are shown in [Figure 13](#). Counterintuitively, CI length also tends to decrease with τ up to $\tau \approx 0.6$, despite the fact that increasing τ reserves less information for inference. This happens when the effect that increasing $|\mathcal{R}|$ has outweighs the increasing variance from the individual signals through the $1 - \tau$ term.

E.2 Simulation results for fixed-design linear regression

The empirical results discussed in 4 demonstrate the advantage of data fission in fixed-design settings with small sample sizes and a handful of points with high leverage. In cases where the sample size is larger and the distribution of covariates are less irregular, data splitting and data fission have roughly similar empirical properties. The following additional simulations help to elucidate this.

Additional metrics In addition to the metrics described in Section 4, we compute two additional metrics to aid in comparison between the available methodologies. In particular, we track the averaged proportion of falsely reported CIs among those indicating a non-zero parameter (the false sign rate),

$$\text{FSR} := \frac{|k \in M : \{\beta_k < 0 \text{ and } \text{CI}_k(1) > 0\} \text{ OR } \{\beta_k > 0 \text{ and } \text{CI}_k(2) < 0\}|}{\max\{|k \in M : 0 \notin \text{CI}_k|, 1\}}, \quad (15)$$

and power of correctly reporting CIs that indicates a nonzero parameter with the correct sign,

$$\text{power}^{\text{sign}} := \frac{|k \in M : \beta_k > 0 \text{ and } \text{CI}_k(1) > 0|}{\max\{|j \in [p] : \beta_j > 0|, 1\}}. \quad (16)$$

In many of the simulations to follow, power, precision, and CI width are almost identical for data splitting and data fission so computing these metrics offer a complementary set of information to aid in performance evaluation.

Simulation with independent covariates We repeat the simulation discussed in Section 4 but now have $p = 100$ features with $x_i \in \mathbb{R}^{100}$. The vector of covariates x_i follows independent standard Gaussians; and $y_i \sim N(\beta^T x_i, \sigma^2)$ where the parameter β is nonzero for 30 features: $(\beta_1, \beta_3, \dots, \beta_{22}, \beta_{92}, \dots, \beta_{100}) = S_\Delta \cdot (\underbrace{1, \dots, 1}_{21}, \underbrace{-1, \dots, -1}_9)$ where S_Δ encodes the signal strength. Figure 14 shows the result of these

simulations averaged over 500 repetitions. Data splitting and data fission appear to have roughly comparable performance in this case, as the large sample sizes allows for data splitting to trade off data between selection and inference smoothly, although the CI lengths are still slightly smaller for data fission.

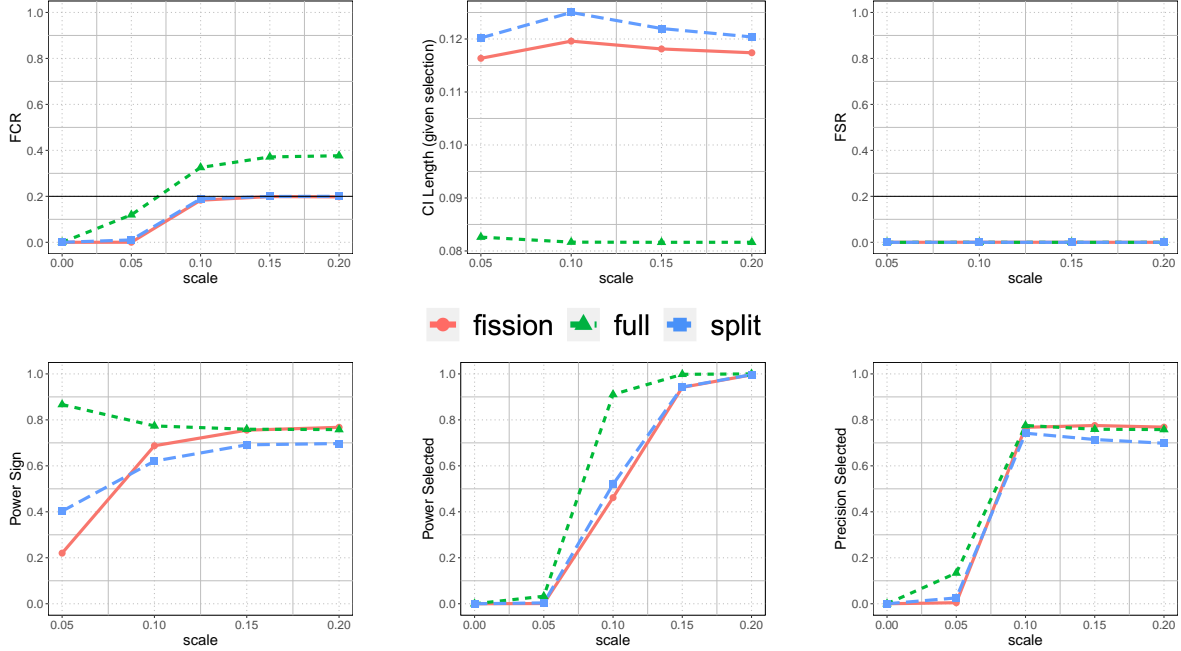


Figure 14. FCR, length of the CIs, FPR and power for the sign of parameters, and power and precision for the selected features, when varying the signal strength S_Δ in $\{0, 0.05, 0.1, 0.15, 0.2\}$. The results are averaged over 500 repetitions. The CIs by using the original data twice do not have FCR control guarantee due to selection bias. In contrast, our proposed procedure using the masking idea has valid FCR, without inflating the length of CIs much or reducing the power of selecting non-zero features.

Simulation with dependent covariates We repeat the experiment described above but with dependent covariates X . We let X be generated from a multivariate Gaussian with zero mean. The covariance matrix is a five-block diagonal matrix, each block a 20×20 Toeplitz matrix:

$$\begin{bmatrix} 1 & \rho & \cdots & \rho^{d-2} & \rho^{d-1} \\ \rho & 1 & \rho & \cdots & \rho^{d-2} \\ \vdots & \vdots & \vdots & \vdots & \vdots \\ \rho^{d-2} & \cdots & \rho & 1 & \rho \\ \rho^{d-1} & \rho^{d-2} & \cdots & \rho & 1 \end{bmatrix}, \quad (17)$$

where $d = 20$. Results are shown in Figure 15 for varying ρ . We note that in this setting the relative ordering of the three methods is unchanged across evaluation metrics, but the power of both data splitting and data fission decreases when there is negative dependence among the covariates.

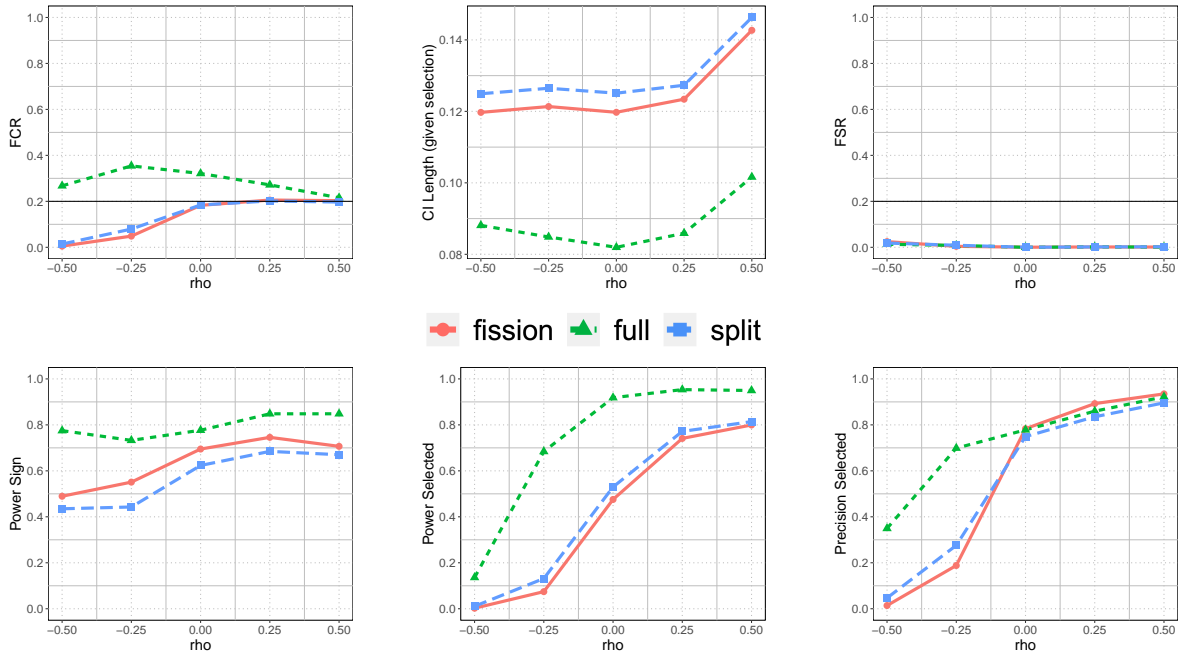


Figure 15. FCR, length of the CIs, FPR and power for the sign of parameters, and power and precision for the selected features, when varying the correlation parameter ρ in $\{-0.5, -0.25, 0, 0.25, 0.5\}$ (with $\rho = 0$ being independent covariates). It appears that negative correlation leads to lower power for all methods.

E.3 Simulation results for fixed-design Poisson regression

We also demonstrate how data fission compare with data splitting in the Poisson regression setting when n is large. Unlike the Gaussian case, the advantages of data fission do not diminish much when used in a large n setting without leverage points. Although we do not have a clear theoretical reason for this result, it is an interesting empirical finding to note as an avenue for future investigation.

Setup. Let y_i be the dependent variable and $x_i \in \mathbb{R}^p$ be a vector of p features. Suppose we have $n = 1000$ samples. We have collected $p = 100$ features $X_i \in \{0, 1\}^2 \times \mathbb{R}^{98}$, where the first two follow $\text{Ber}(1/2)$ and the rest follow independent Gaussians. Suppose Y_i follow a Poisson distribution with the expected value $\exp\{\beta^T X_i\}$, where the parameter β is nonzero for 29 features: $(\beta_1, \beta_3, \dots, \beta_{22}, \beta_{93}, \dots, \beta_{100}) = S_\Delta \cdot (\underbrace{1, \dots, 1}_{21}, \underbrace{2, \dots, 2}_8)$ and S_Δ encodes the signal strength.

Simulation results with mutually independent covariates. As an illustration of the procedure, Figure 16 shows an instance of selected features and the constructed CIs for a single trial run. The selected features are marked by blue crosses, which include all of the nonzero coefficients (corresponding to almost 100% power for selection) and also many zero coefficients (corresponding to around 50% precision for selection). The constructed CIs that do not contain the true value are marked in red.

Figure 17 shows results averaged over 500 trials. Compared with the results using data splitting, the CI using data fission is significantly tighter. Although the precision during the selection step is not high for both methods (around 50% of selected features do not have true signals), we are able to identify the true signals by constructing CIs in the second step with FCR control. When interested in the sign indicated by the CIs, we have constructed CIs indicating a positive sign for all of the nonzero (in our case positive) coefficients (reflected as 100% power for the signs and 0% FSR).

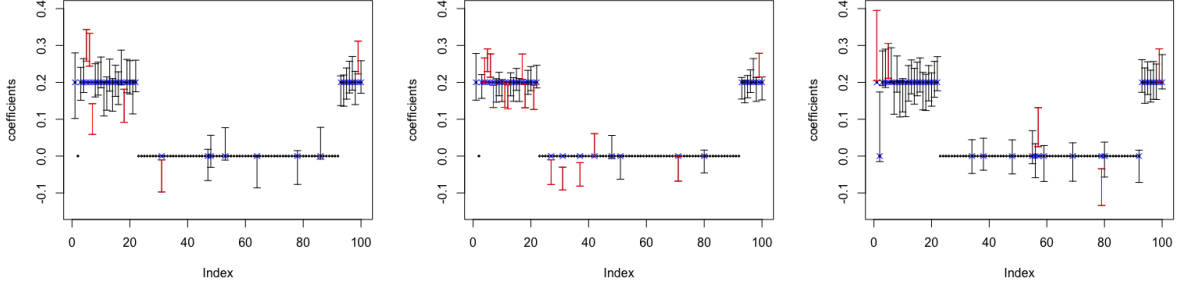


Figure 16. An instance of the selected feature (blue crosses) and the constructed CIs using fissioned data (left), full data twice (middle), and split data (right). CIs which do not cover the parameters correctly are marked in red.

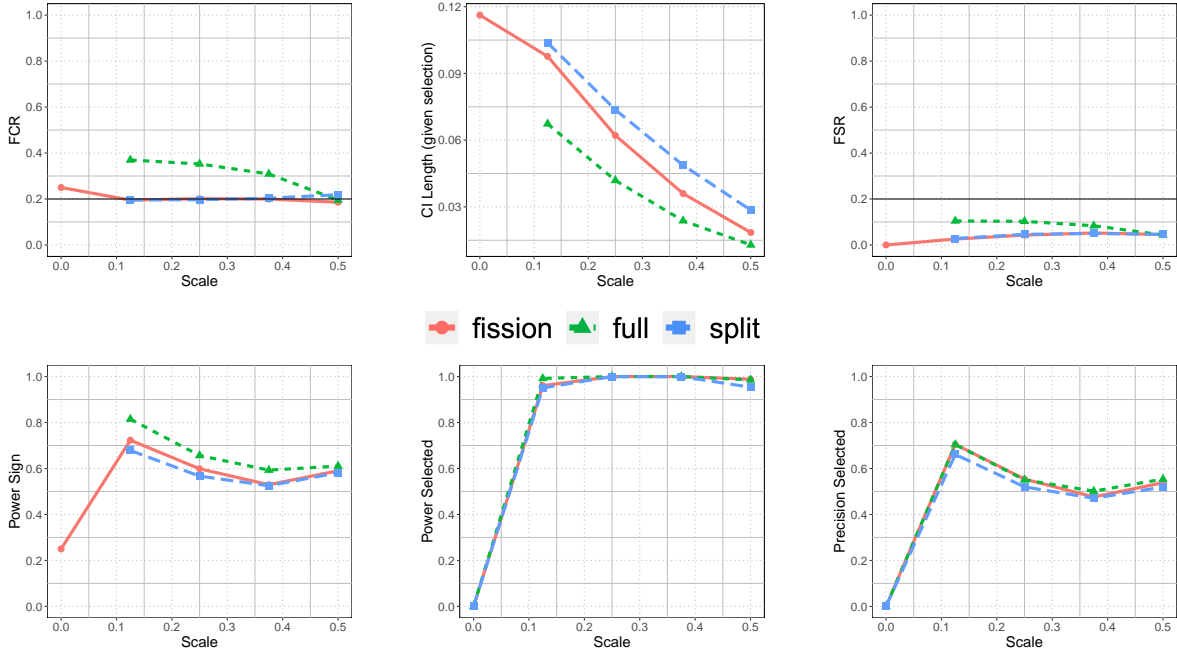


Figure 17. FCR, length of the CIs, FPR and power for the sign of parameters, and power and precision for the selected features, when varying the signal strength S_{Δ} in $\{0, 0.125, 0.25, 0.375, 0.5\}$. The results are averaged over 500 repetitions. The CIs by using the original data twice do not have FCR control guarantee due to selection bias. In contrast, our proposed procedure using fission has valid FCR, without inflating the length of CIs much or reducing the power of selecting non-zero features.

Simulation results with dependent covariates. We modify the above simulation slightly so that the X are samples from *dependent* rather than independent Gaussians. The covariance matrix is a five-block diagonal matrix, each block a 20×20 toeplitz matrix:

$$\begin{bmatrix} 1 & \rho & \cdots & \rho^{d-2} & \rho^{d-1} \\ \rho & 1 & \rho & \cdots & \rho^{d-2} \\ \vdots & \vdots & \vdots & \vdots & \vdots \\ \rho^{d-2} & \cdots & \rho & 1 & \rho \\ \rho^{d-1} & \rho^{d-2} & \cdots & \rho & 1 \end{bmatrix}, \quad (18)$$

where $d = 20$. Results averaged over 500 trials are shown in Figure 18 for varying ρ .

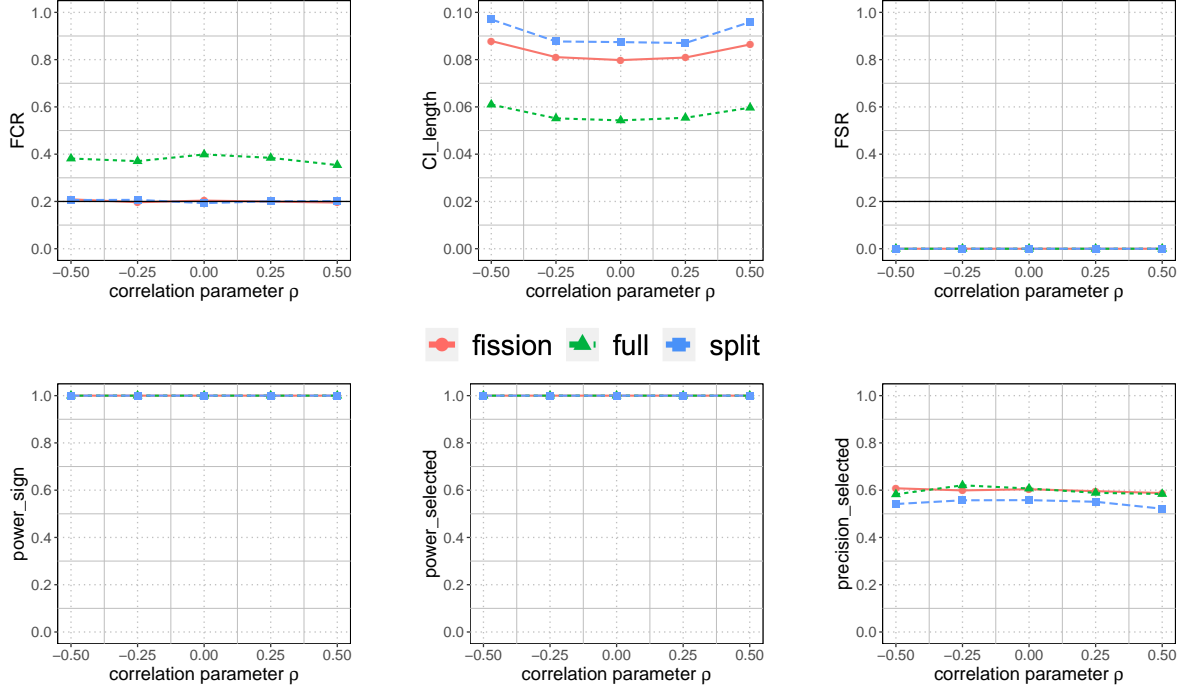


Figure 18. FCR, length of the CIs, FSR/power for the sign of parameters, and power and precision for the selected features, when varying the correlation parameter ρ in $\{-0.5, -0.25, 0, 0.25, 0.5\}$ (with $\rho = 0$ corresponding to mutually independent covariates). The performance of the three methods is relatively similar under different degrees of dependence.

Data fission continues to have tighter confidence intervals than data splitting, though the performances across the three methods are similar for the other metrics.

E.4 Simulation results for fixed-design logistic regression

We also explore the empirical performance of data fission in a logistic regression setting.

Setup. Let y_i be the dependent variable and $x_i \in \mathbb{R}^p$ be a vector of p . We let $n = 1000$ and $p = 100$ with $x_i \in \{0, 1\}^2 \times \mathbb{R}^{98}$ generated with a $\text{Ber}(1/2)$ for the first two entries and the remaining following iid Standard Gaussians. Suppose the conditional distribution of y_i given x_i is a Bernoulli distribution with expected value $(1 + \exp\{-\beta^T x_i\})^{-1}$, where the parameter β is nonzero for 30 features: $(\beta_1, \beta_3, \dots, \beta_{22}, \beta_{92}, \dots, \beta_{100}) = S_\Delta \cdot \underbrace{(1, \dots, 1)}_{21}, \underbrace{2, \dots, 2)}_9$ and S_Δ encodes the signal strength.

Proposed procedure. Following Section 2.2, we can use data fission for constructing selective CIs as follows.

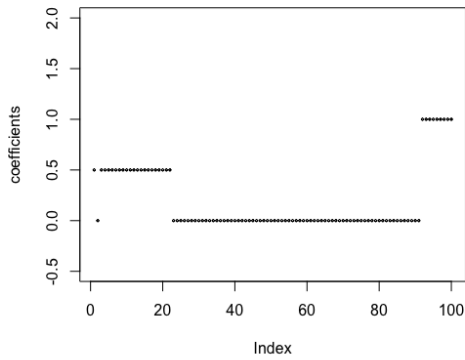
1. Draw $Z_i \sim \text{Ber}(p)$ where the “flip probability” $p \in (0, 1)$ is a tuning parameter; and let $f(Y_i) = Y_i(1 - Z_i) + (1 - Y_i)Z_i$, and $g(Y_i) = Y_i$.
2. Fit $f(Y_i)$ with a GLM with a logit link function and lasso regularization to select features, denoted as $M \in [p]$ (in our examples, we use `cv.glmnet` in the R package `glmnet` and choose

the tuning parameter λ by the 1 standard deviation rule, which can be found in the value of `lambda.1se`).

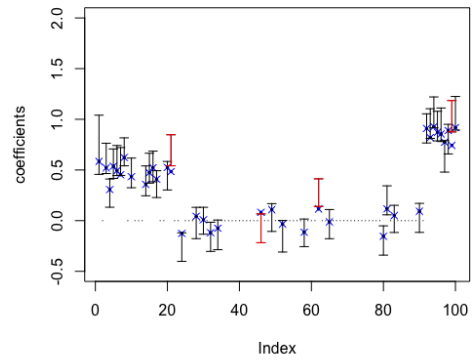
3. Fit $g(Y_i)$ with another GLM with a logit link function and no regularization using *only* the selected features (we use `glm` in the R package `stats`).
4. Construct CIs for the coefficients trained in the third step, each at level α and with the standard errors estimated as in [Theorem 5](#). For the experiments shown below, we also apply a finite sample correction as described in [Pustejovsky and Tipton \(2018\)](#).

For greater detail on steps 3 and 4, see the logistic regression discussion in [Appendix A.5](#). Since the working model is not correctly specified in instance, the CIs are now covering the target parameters $\beta_n^*(M)$ which minimize the KL divergence between the chosen model and the true distribution of the data.

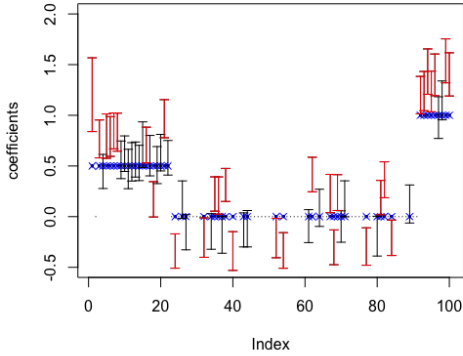
This procedure is illustrated for a single trial run in [Figure 19](#). As usual, we compare the CIs constructed using data fission with data splitting and the (invalid) approach of reusing the full dataset for both selection and inference.



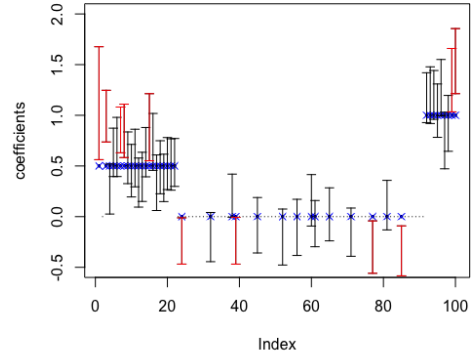
(a) True coefficient values.



(b) CI for target parameters using data fission.



(c) CIs for target parameters using full data twice.



(d) CIs for target parameters using splitting.

Figure 19. An instance of CIs for an example set of selected features using data fission, data splitting, and the (invalid) approach of using using the full dataset twice for both selection and inference. The upper left-hand graph shows the true coefficients, but the CI cover the target parameters as described above. However, the target parameters are quite close to the original coefficient values in this instance (as well as most instances encountered in simulation). We note that both data splitting and data fission have valid FCR control (at target level = 0.2), but the CIs constructed using data fission are much tighter.

Simulations varying signal strength. We repeat this experiment over 500 trials while varying signal strength from 0 to 0.5, with results shown in Figure 20. We note that across all observed signal strengths, data fission offers tighter CIs when compared to both data splitting *and* the (invalid) approach that reuses the full dataset for both selection and inference. This is a remarkable feat since it is typically the case (e.g. in the Gaussian and Poisson applications of data fission) that larger CIs are the price that is required in order to ensure coverage guarantees. Although we do not have a precise explanation for this phenomenon, it may be due to the misspecification that results from data fission recasting the target parameters into something “easier” to estimate.

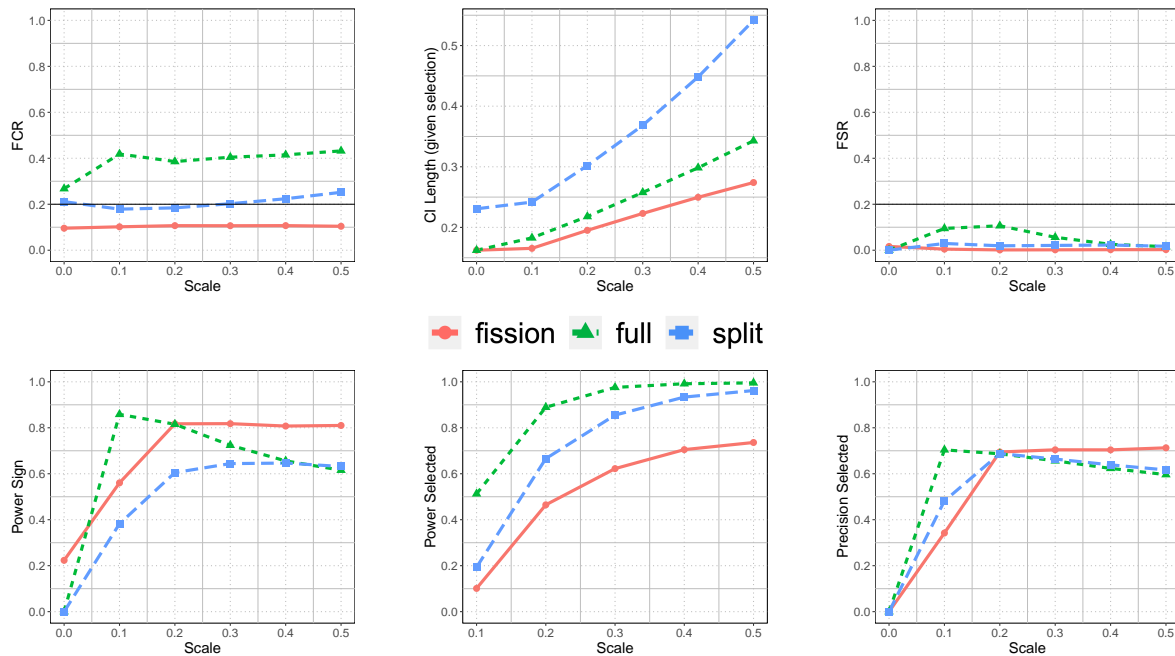


Figure 20. FCR, CI width, FSR, power for the sign of parameters, and power and precision for the selected features, when varying the signal strength S_Δ in $\{0, 0.1, 0.2, 0.3, 0.4, 0.5\}$. The hyperparameter p is chosen as 0.2 and target FCR for CIs is set at 0.2. We note that data fission offers smaller CI widths when compared to both data splitting and the (invalid) approach that reuses the full dataset for both selection and inference.

Simulations varying fission hyperparameter p . We also examine the performance of these experiments as we vary the fission hyperparameter p . We note that values of p close to either 0 or 1 correspond to having more information reserved for the selection step, while setting $p = 0.5$ maximizes the amount of information reserved for inference. In Figure 21, we can see this behavior manifested in the “dips” in the CI length, power and precision as p ranges from 0.3 to 0.5.

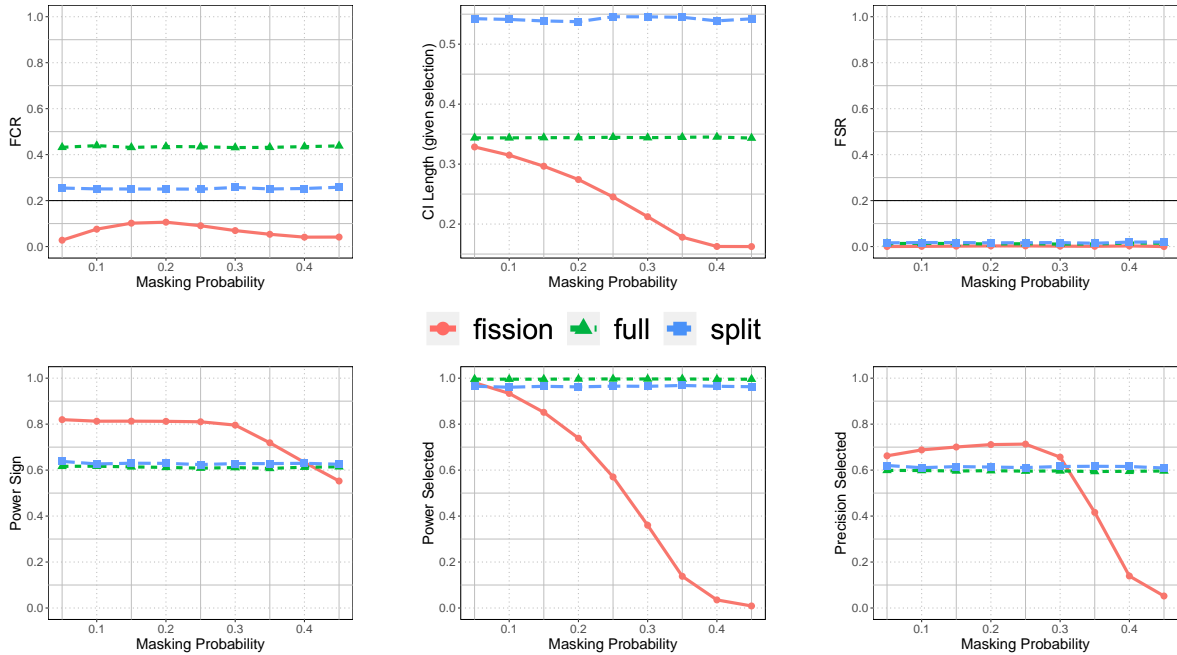


Figure 21. FCR, CI width, power for the sign of parameters, and power/precision for the selected features, when varying the hyperparameter p in $\{0.05, 0.1, 0.15, 0.2, 0.25, 0.3, 0.35, 0.4, 0.45\}$ with fixed signal strength $S_\Delta = 0.5$. The power and precision are higher when p is closer to either 0 or 1 rather than 0.5. Interestingly, however, the CI lengths only slightly increases as p varies away from 0.5.

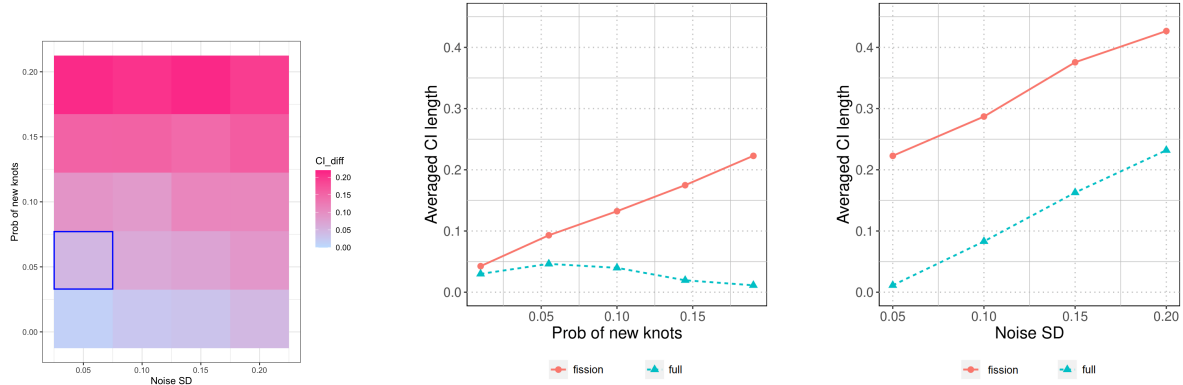
E.5 Simulation results for trend filtering

This section contains supplemental results for Section 6. In particular:

- In Section 6.1, we note that data fission enables the construction of confidence intervals with proper pointwise and uniform coverage but at the price of wider confidence intervals when compared with using the full dataset twice for selection and inference. In Appendices E.5.1 and E.5.2, we investigate how the confidence intervals compare between these two methods.
- In Appendix E.5.3, we investigate an extension of the trend filtering methodology that accounts for unknown variance.
- In Appendix E.5.4, we investigate alternative ways of selecting knots apart from cross validation such as Stein’s unbiased risk estimate (SURE).

E.5.1 Additional results for pointwise CI simulations

In addition to FCR, we also track the pointwise CI length for the simulations described in Section 6.1. We see that when using the full data twice, the average CI length shrinks drastically when the probability of new knots increases while data fission enforces confidence intervals that grow in size as the number of knots increases. In contrast, when the underlying variance increases, both methods increase the length of the confidence intervals.



(a) Difference in the averaged CI length when reusing the full dataset, versus data fission.

(b) CI lengths when noise SD is 0.05.

(c) CI lengths when the probability of new knots is 0.2.

Figure 22. The width of **pointwise CIs** when varying the probability of having knots p in $\{0.01, 0.55, 0.1, 0.145, 0.19\}$ and the noise SD in $\{0.05, 0.1, 0.15, 0.2\}$. The widths for CIs constructed using data fission range from 0.03 to 0.43, and are larger than the CIs constructed when the full dataset is reused for inference. Both methods have increased CI length as the noise SD increases, but when reusing the full dataset, the length is still not adequate to ensure FCR control. Interestingly, only the data fission approach increases the length of the CI as the number of knots increases.

E.5.2 Additional results for uniform CI simulations

In addition to simultaneous type I error control, we also track the uniform CI length for the simulations described in Section 6.1 in Figure 23. The differences between CIs constructed using data fission and using the full dataset twice are most stark when the noise is small and the probability of new knots is large because these are the circumstances where the trend constructed using the full dataset is likely to overfit.

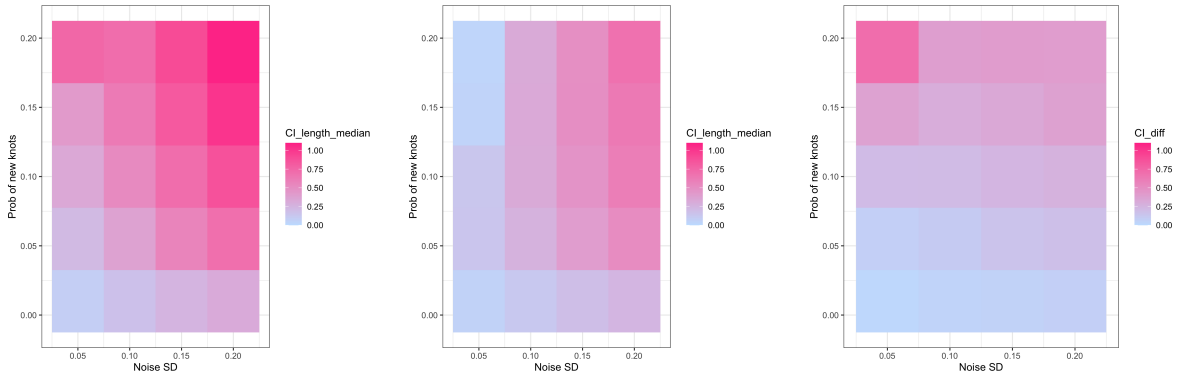


Figure 23. The median CI width using either data fission (left) or full data twice (middle) for **uniform CIs** have similar trends with respect to noise SD and probability of new knots. The CI difference (fission CI minus full-data CI) decreases when the noise SD increases (such that the effect of double dipping is smaller) or the probability of new knots decreases. These settings also correspond to instances where reusing the full dataset twice tends not violate FCR or type I error control too badly, since the width of the intervals is almost the same as those created from data fission.

Understanding the relationship of $c(\alpha)$ to changing CI lengths One obstacle in understanding how the widths of uniform confidence bands change as noise increases and the underlying structural trend changes is that the length is controlled by the multiplier $c(\alpha)$ used in Fact 1 which is somewhat opaque. Recall that $c(\alpha)$ is the solution to

$$\frac{|\gamma|}{2\pi} e^{-c^2/2} + 1 - \Phi(c) = \alpha/2. \quad (19)$$

To aid in forming an intuition behind the empirical trends noted in Figure 23, we plot some intermediate statistics in Figure 24.

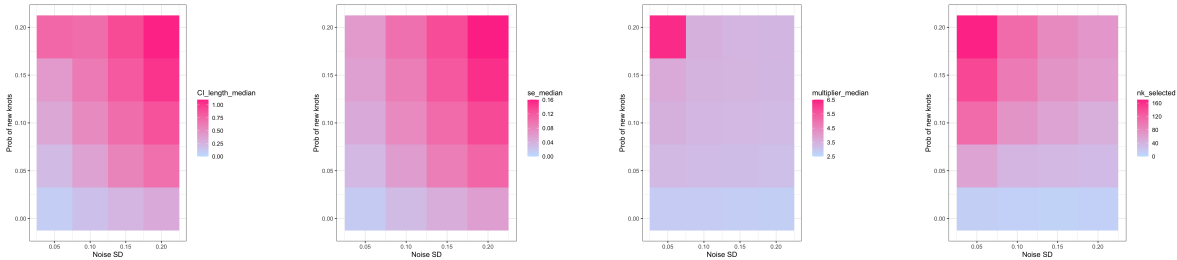
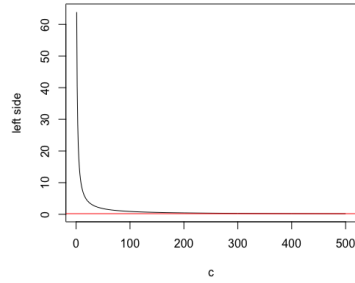


Figure 24. The CI width using data fission method increases with noise variance and the probability of new knots (first), because \widehat{SE} increases (second) compared to the change in the multiplier $c(\alpha)$ (third). Both changes can be traced back to change in the number of knots (fourth): \widehat{SE} decreases and $c(\alpha)$ increases with the number of knots.

The above plots are medians over repetitions since the distribution of CI width is skewed to large values; thus, the mean may not summarize the pattern clearly. The mean of CI width does not have a consistent trend because there are a few extremely large CI widths, due to extremely large multipliers $c(\alpha)$. Upon closer inspection, such large value exist when the number of knots is large. In Figure 25, we show the value of left-hand side of (19) for solving $c(\alpha)$ when the number of knots is 197 (vs 200 time points). The solution for $c(\alpha)$ is over 400 (at the intersection of the black path and the red level of α).



(a) Trajectory of the left-hand side of (19) when there are 197 knots.



(b) Log of the multiplier when the number of knots increases from 190 to 197.

Figure 25: The multiplier $c(\alpha)$ increases dramatically when the number of knots is larger than 190.

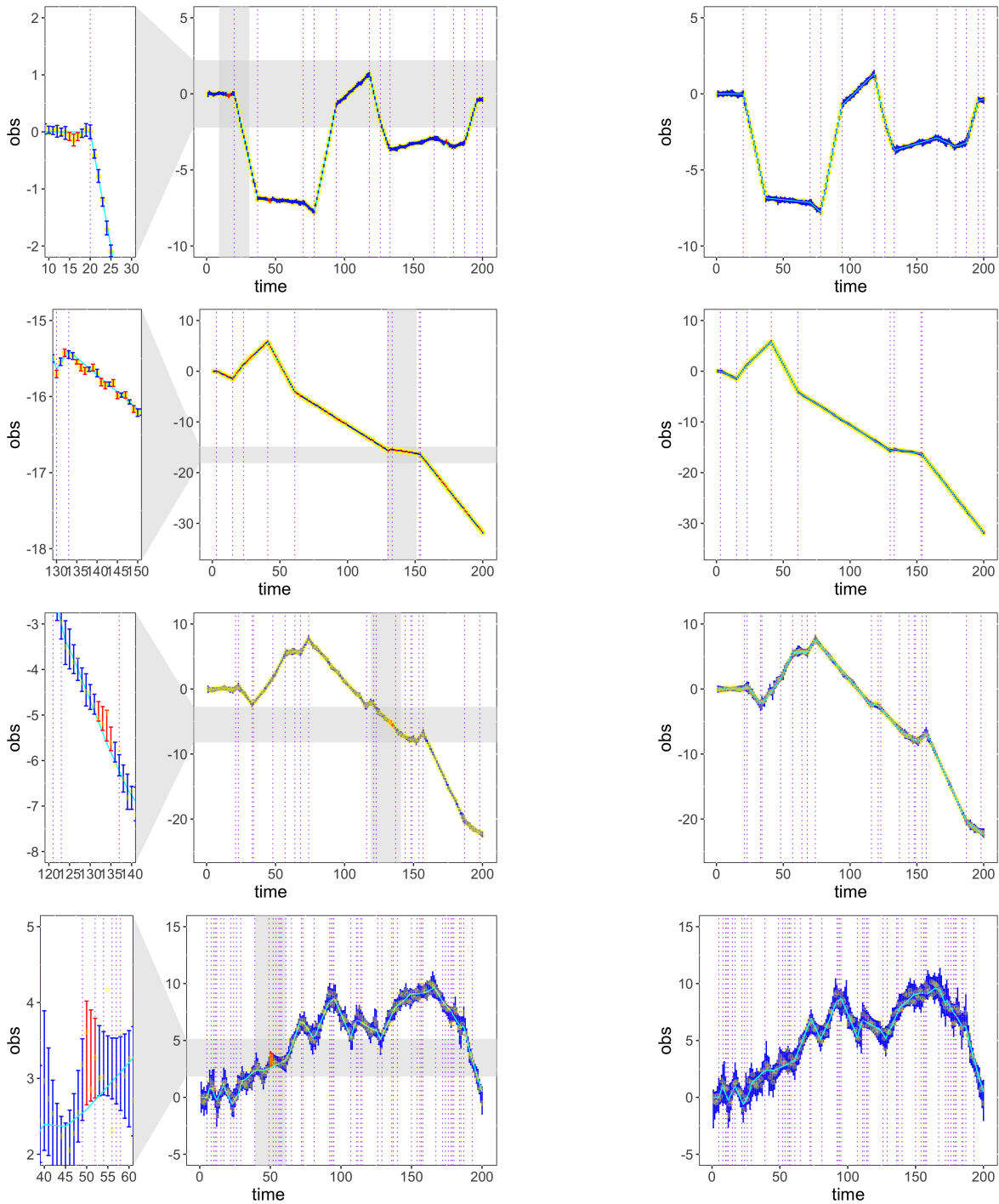


Figure 26. Four instances of the observed points (in yellow) and the *uniform* CI (in blue if correctly cover the trend, in red if not) using two types of methods: full data twice (left), and data fission (right). The underlying projected mean is marked in cyan, which also mostly overlaps with the original true trend because both methods can find turning points easily under small noise.

Example trials for uniform confidence bands Similar to the examples shown in Figure 9, we visualize the coverage of uniform confidence bands as well over four examples in Figure 26. The CI using the full data fails to cover the projected mean at many time points because of double dipping, whereas data fission leads to a uniformly-valid CI with type I error control.

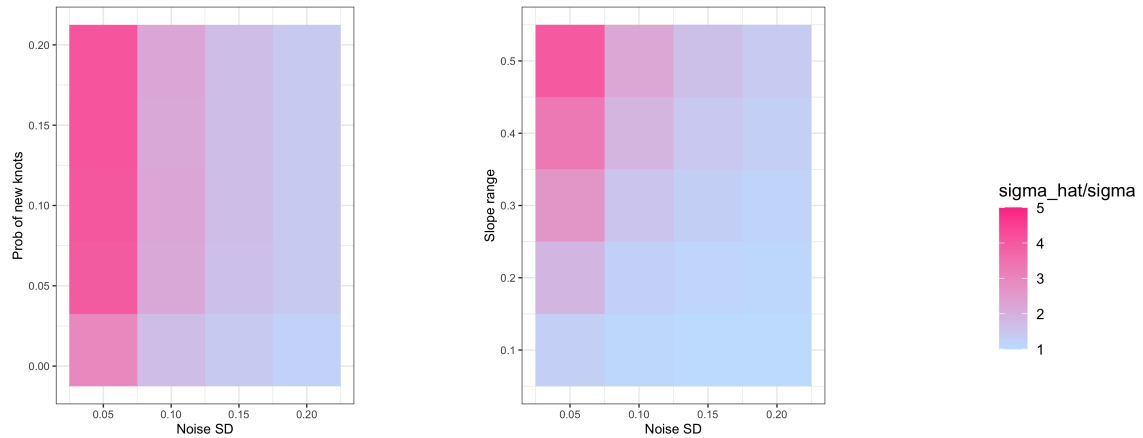
E.5.3 Estimating variance before data fission

The procedure discussed in Section 6 uses the knowledge of variance σ^2 , which is usually not known in practice. Alternatively, we can estimate the variance as $\hat{\sigma}^2 = \frac{1}{2(n-1)} \sum_{i=1}^{n-1} (y_{t+1} - y_t)^2$ before step 1, and simulate $z_t \sim N(0, \hat{\sigma}^2)$. We must also modify equation (19) in step 4 slightly by replacing it with equation (5.6) in Koener (2011) and instead choose $c(\alpha)$ to be the solution of

$$\frac{|\gamma|}{2\pi} (1 + c^2/v)^{-v/2} + P(t_v > c) = \alpha/2 \quad (20)$$

where t_v denotes a t -distribution with $v = n - m - 1$ degrees of freedom with m being the number of knots.

Notice that because we use the observed data to estimate variance, it could break the independence between $f(Y)$ and $g(Y)$. However, we notice in simulation that the error control still seems to hold in most cases. First, we evaluate how well the variance can be estimated across different settings in Figure 27. The proposed methodology tends to overestimate the noise SD in general, with this overestimation increasing as the probability of new knots increases or the slope increases, because the formula to compute $\hat{\sigma}^2$ given above treats all the change in adjacent time points as noise.

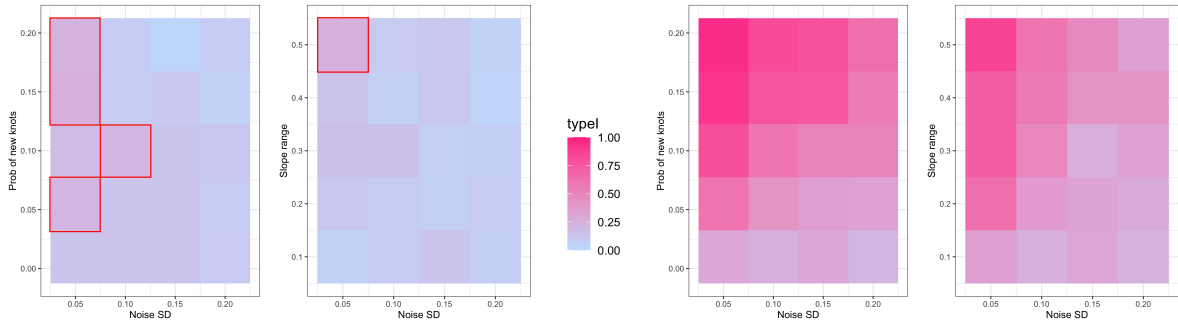


(a) Vary the true variance and prob of new knots when fix the slope range as 0.5.

(b) Vary the true variance and slope range when fix the prob of new knots as 0.1.

Figure 27. The noise SD is often over estimated with a range in (0.05, 0.3) and the true one varies in (0.05, 0.2). The over-estimation fades when the noise SD increases and the slope decreases (and slightly fades as the probability of new knots decreases).

Luckily, a tendency to overestimate the variance leads to conservative CIs, meaning errors are still controlled at the appropriate level in most cases. We see in Figure 28 that data fission still offers simultaneous type I error control empirically when using uniform confidence bands. This is achieved at the expense of having overly conservative CIs in cases where the underlying structural trend is variable — either because of many knots points or because of the size of the slope. We investigate how the level of conservatism, as measured by the average widths of the constructed confidence bands, increases as the underlying trend varies more in Figure 29.



(a) Data fission method when varying prob of new knots. (b) Data fission method when varying slope range. (c) Full data twice when varying prob of new knots. (d) Full data twice when varying slope range.

Figure 28. Simultaneous type I error for the uniform CI constructed using data fission, and full data twice, when varying the probability of new knots, the slope range, and the true noise variance. Data fission method seems to have lower simultaneous type I error than the target level (0.2) in most cases, except cases circled in red (with a max simultaneous type I error of 0.26).

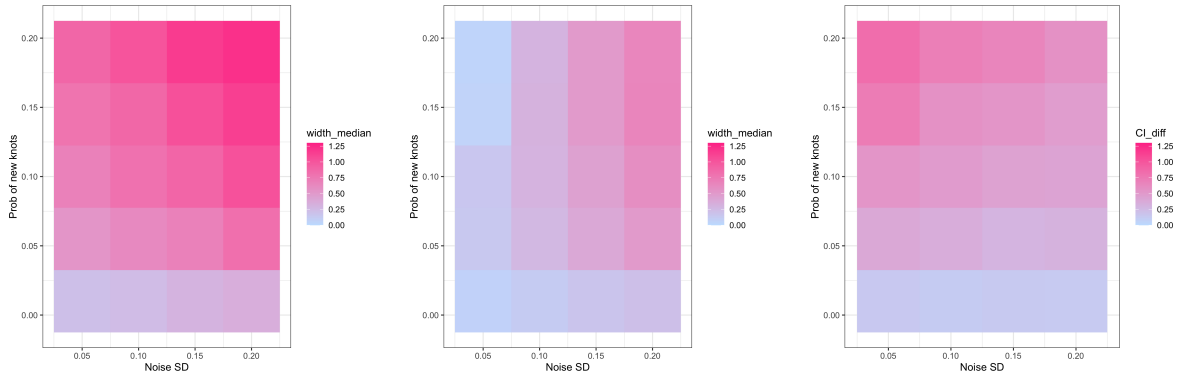


Figure 29. The CI width for uniform confidence bands using either data fission (right) or full data twice (left) have similar trends with respect to noise SD and probability of new knots. The difference in CI length between the two methods decreases when the noise SD increases (such that the effect of double dipping is smaller) or the probability of new knots gets smaller (such that the CI from data fission is tighter).

E.5.4 Alternative methods for selecting knots

In Section 6.1, we selected the knots by choosing the regularization parameter with the smallest cross-validation error, which often leads to selecting more knots than the underlying truth when the full dataset is used for both selection and inference. Although data fission allows for an analyst to guarantee error control under arbitrary selection rules, some selection rules tend to be more robust to the analyst reusing the data in terms of their empirical performance even if statistical guarantees are not available.

Stein’s unbiased risk estimate (SURE) An alternative methodology for selecting knots would be to minimize the SURE formula — which provides an unbiased estimate of mean-squared percentage error in a fixed-design setting. In the context of trend filtering, this can be computed as

$$\frac{1}{n} \sum_{i=1}^n (y_i - \hat{\mu}_i)^2 + 2\sigma^2 \frac{m}{n}$$

where m is the number of knots chosen to fit $\hat{\mu}$. Interestingly, using this formula seems to result in type I error being controlled even when reusing the full data for both selection and inference. Please see [Politsch et al. \(2020a\)](#) for further background on how SURE can be used to aid in knot selection.

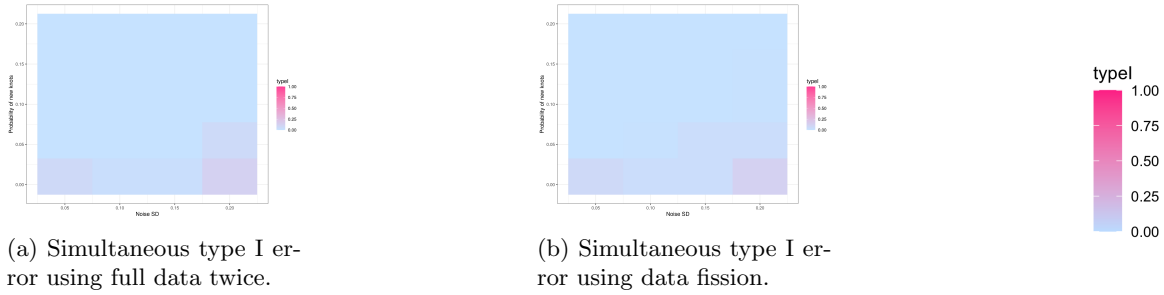


Figure 30. Simultaneous type I error for **uniform CIs** as we vary the probability of having new knots $q \in \{0.01, 0.55, 0.1, 0.145, 0.19\}$ and the noise SD in $\{0.05, 0.1, 0.15, 0.2\}$. The error control violation when using the full data twice is no longer as stark in the simulation results when using SURE as the selection rule, with the highest simultaneous type I error at 0.2 given target level $\alpha = 0.2$.

1-SD Rule To mitigate the possibility of over selection of knots, an alternative approach is to choose the regularization parameter to be the one with smallest error plus one standard deviation. As we observe in [Figure 31](#), adding a standard deviation to the selection rule does not change the error much. However, this rule appears to be more robust when the full data is reused for inference—in [Figure 32](#), we can see that simultaneous type I error control is not as seriously violated when using this selection rule.

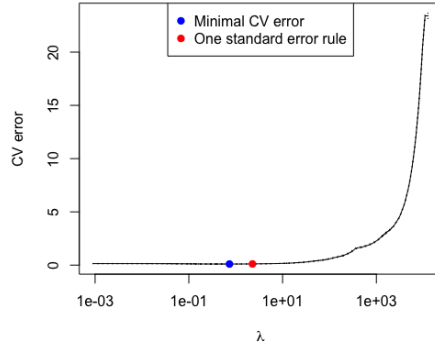
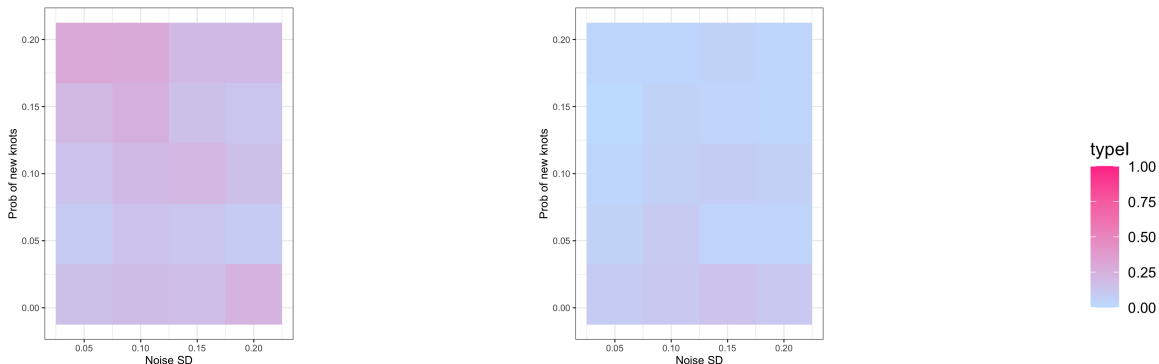


Figure 31. In the path of regularization parameter, adding an extra standard deviation does not change the error much.



(a) Simultaneous type I error using full data twice.

(b) Simultaneous type I error using data fission.

Figure 32. Simultaneous type I error for **uniform CIs** as we vary the probability of having new knots $q \in \{0.01, 0.55, 0.1, 0.145, 0.19\}$ and the noise SD in $\{0.05, 0.1, 0.15, 0.2\}$. The error control violation when using the full data twice is no longer as stark in the simulation results when using this new selection rule, with the highest simultaneous type I error at 0.3 given target level $\alpha = 0.2$.

F Additional empirical results for spectroscopy datasets

We show results in this section for the remaining astronomical objects of interest described in [Section 6.2](#).

1. A **galaxy**. DR12, Plate= 7140, MJD = 56569, Fiber=68. Located at (RA,Dec, z) $\approx (349.374^\circ, 33.617^\circ, 0.138)$. Results shown in [Figure 33](#).
2. A **star**. DR12, Plate= 4055, MJD = 55359, Fiber=84. Located at (RA,Dec, z) $\approx (236.834^\circ, 0.680^\circ, 0.000)$. Results shown in [Figure 34](#).

As a point of comparison, we use quadratic rather than linear trend filtering to model these spectra. We note an interesting tradeoff between the degree of the polynomial that is used and the smoothness of the estimated function. Larger degree polynomial result in fewer knots being chosen during the selection step which leads to a smoother-looking confidence band, but at the expense of not capturing some of the more volatile pieces of the data. Smaller degree polynomials results in more knots being chosen during the selection stage which leads to a less smooth band but also a function that tracks the overall volatility of the data more closely.

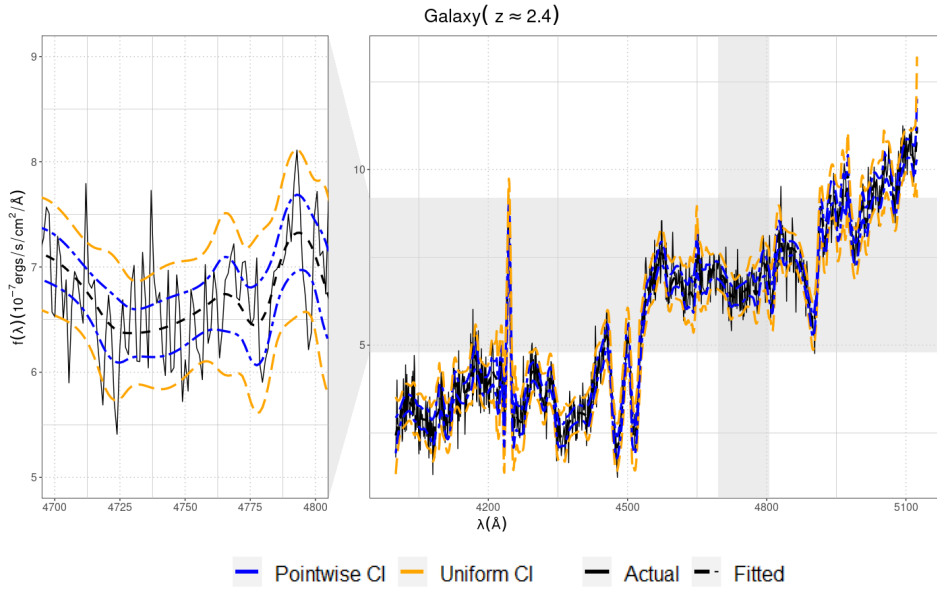


Figure 33. Fitted values using quadratic trend filtering as well as uniform and pointwise CIs for a **galaxy**. DR12, Plate= 7140, MJD = 56569, Fiber=68. Located at (RA,Dec, z) \approx (349.374°, 33.617°, 0.138).

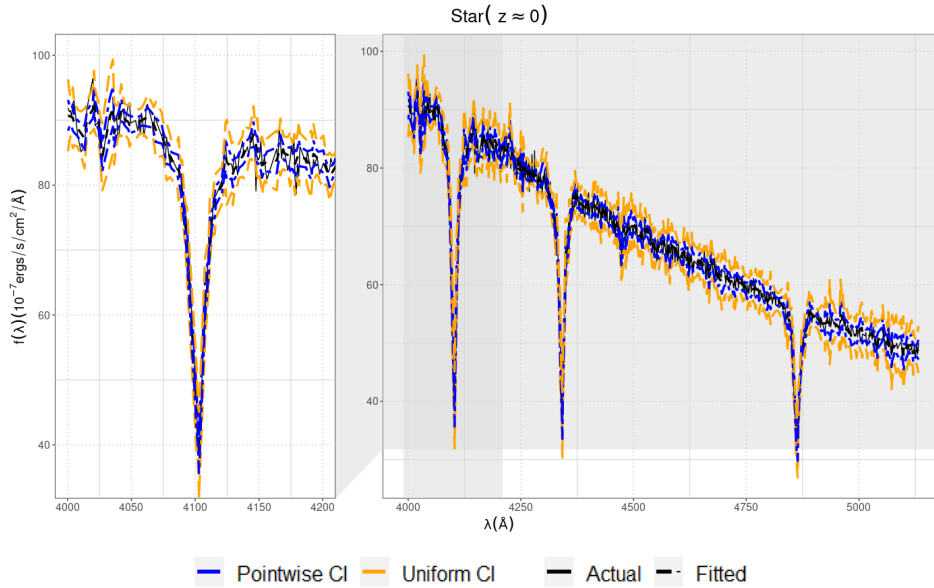


Figure 34. Fitted values using quadratic trend filtering as well as uniform and pointwise CIs for a **star**. DR12, Plate= 4055, MJD = 55359, Fiber=84. Located at (RA,Dec, z) \approx (236.834°, 0.680°, 0.000).